

Computation of quark mass anomalous dimension at $O(1/N_f^2)$ in quantum chromodynamics

M. Ciuchini^a, S.É. Derkachov^{b*}, J.A. Gracey^{a†} & A.N. Manashov^{c‡}

^a Theoretical Physics Division, Department of Mathematical Sciences,
University of Liverpool, Liverpool, L69 7ZF, United Kingdom.

^b Institut für Theoretische Physik, Universität Leipzig,
Augustusplatz 10, D-04109 Leipzig, Germany &
Department of Mathematics, St Petersburg Technology Institute,
Sankt Petersburg, Russia

^c Institut für Theoretische Physik, Universität Regensburg,
D-93040 Regensburg, Germany &
Department of Theoretical Physics, State University of St Petersburg,
Sankt Petersburg, 198904 Russia.

Abstract. We present the formalism to calculate d -dimensional critical exponents in QCD in the large N_f expansion where N_f is the number of quark flavours. It relies in part on demonstrating that at the d -dimensional fixed point of QCD the critical theory is equivalent to a non-abelian version of the Thirring model. We describe the techniques used to compute critical two and three loop Feynman diagrams and as an application determine the quark wave function, η , and mass renormalization critical exponents at $O(1/N_f^2)$ in d -dimensions. Their values when expressed in relation to four dimensional perturbation theory are in exact agreement with the known four loop $\overline{\text{MS}}$ results. Moreover, new coefficients in these renormalization group functions are determined to six loops and $O(1/N_f^2)$. The computation of the exponents in the Schwinger Dyson approach is also provided and an expression for η in arbitrary covariant gauge is given.

*e-mail: Sergey.Derkachov@itp.uni-leipzig.de

†e-mail: jag@amtp.liv.ac.uk

‡e-mail: manashov@heps.phys.spbu.ru

1 Introduction.

Recent developments in the area of multiloop calculations in quantum chromodynamics, (QCD), have included the determination of the $\overline{\text{MS}}$ four loop β -function, [1], and the four loop quark mass anomalous dimension, [2, 3]. These calculations involved current state of the art analytic and symbolic manipulation techniques in the evaluation of the order of 10,000 Feynman diagrams. Such high order calculation are necessary to refine our understanding, for example, of the running of the quark masses, [2, 3]. Indeed such four loop calculations have built on the early lower order work of *several* decades of [4, 5, 6, 7, 8] for the QCD β -function and [9, 10, 11] for the quark mass anomalous dimension. Whilst we believe the results of [1] and [2, 3] will not be superseded by a five loop calculation for quite some time, it is possible to probe the higher order structure of the QCD renormalization group, (RG), functions using techniques alternative to conventional perturbation theory. One such approach is the large N_f expansion where N_f is the number of quark flavours. In this method the Feynman diagrams contributing to the determination of an RG function are reordered according to the number of quark loops and evaluated by considering at leading order those graphs which are simply a chain of bubbles. The next order is represented by those bubble chains which have either one vertex or self energy correction and so on. Clearly this large N_f reordering will cover the information already contained in explicit perturbative loop calculations but will reveal new information beyond the current orders. For simple scalar field theories such as the $O(N)$ ϕ^4 theory or the $O(N)$ nonlinear σ model, the large N technique has been developed to determine information on the RG functions at $O(1/N^3)$, [12, 13]. That impressive programme of Vasil'ev et al exploited ideas from critical renormalization group theory and determined rather than the RG functions themselves, the related critical exponents. These correspond to the RG functions evaluated at the d -dimensional fixed point of the β -function which in $O(N)$ ϕ^4 theory is the Wilson-Fisher fixed point. The techniques developed in the early work on scalar theories, [12, 13, 14], have been applied to QCD at leading order in $1/N_f$ in [15, 16]. Further, information on the anomalous dimension of the twist-2 operators fundamental to the operator product expansion used in deep inelastic scattering has been produced as a function of the operator moment, [17]. Although it is important that these calculations are extended to next order in $1/N_f$, it turns out that there are several issues which need to be addressed. First, no rigorous proof exists of the critical equivalence of QCD and the so called nonabelian Thirring model, (NATM), which underlies all the large N_f computations. The original observation of the connection between the models in [18] was effectively at $O(1/N_f)$. Second, the analytic regularization commonly used in $1/N$ calculations breaks the gauge invariance of the theory. As far as we are aware all other regularizations spoil the masslessness of the propagators and this therefore makes higher order calculations virtually impossible. We note that dimensional regularization, which is ordinarily used in conventional perturbation theory, is not applicable in large N_f work since the theory remains divergent in arbitrary dimensions. This second obstacle is much more serious and might seem to destroy the possibility of developing a sensible $1/N_f$ scheme. The resolution of the issues of the proof of the critical equivalence of QCD and the NATM as well as demonstrating that the critical exponents evaluated in the latter model using non-gauge invariant regularizations do in fact match those of QCD are of extreme importance and represent the central results of this paper. By way of application and in order to support the scheme which will be developed in practical calculations we examine the quark and mass anomalous dimensions and determine them at new order in the large N_f expansion which is $O(1/N_f^2)$. A preliminary version of our results was given in [19].

There are various motivations for examining these two RG functions. First, as in conventional perturbation theory one always needs to deduce the wave function renormalization of the fundamental fields of a theory before considering the renormalization of the other parameters

and operators in a Lagrangian. Likewise in the large N_f approach the evaluation of the wave function exponent, η , needs to be determined first. Indeed in the context of the phenomenological application of the large N_f technique the programme of evaluating anomalous dimensions of the twist-2 operators of deep inelastic scattering at $O(1/N_f^2)$ cannot proceed prior to the determination of η at the same order. Second, although η is fundamental it depends on the covariant gauge parameter introduced in the gauge fixing of the NATM Lagrangian. Consequently, it is not as fundamental a quantity as a gauge independent exponent. Therefore, to further understand the large N_f method in QCD at $O(1/N_f^2)$ we have undertaken to consider the gauge independent quark mass anomalous dimension. Indeed as part of our calculations we address the issue of the choice of gauge in the large N_f method. Whilst it may seem that the evaluation of two exponents at $O(1/N_f^2)$ is a formidable task, it turns out that the computation of the quark mass dimension does not represent a significant amount of additional calculation as there is, in fact, a close relation between the fermionic graphs for the wave function and mass dimension which we will establish.

It is worth noting that our detailed calculation relies on the novel method of [20, 21] for the computation of critical exponents in $1/N$ expansion. In comparison with the standard technique [12] based on the direct solution of the Schwinger-Dyson (SD) equations the latter approach allows us to express the critical exponents through the corresponding renormalization constants whose explicit form is very similar to those computed using dimensional regularization. The immediate advantage is that it allows one to use techniques similar to the infra-red rearrangement of conventional high order perturbative calculations to evaluate the three loop critical point Feynman diagrams needed for the present calculation. This approach, which was originally developed to analyse the $O(N)$ nonlinear σ model appears to be universal, and can be easily extended to the case we will consider. Together with some calculational shortcuts it makes the evaluation of almost all the relevant graphs quite straightforward and simplifies computations significantly. In addition we will also present the Schwinger-Dyson formalism for the determination of η at $O(1/N_f^2)$ in QCD. This builds naturally on the earlier large N_f calculations in quantum electrodynamics, (QED), [22, 23, 24]. In those papers the original technique of [12] in solving the SD equations was followed and in extending the formalism to QCD here will provide an interested reader with a unique opportunity to compare both approaches. Finally, it is worth stressing that the consistency of our final results for the quark and mass anomalous dimensions at $O(1/N_f^2)$ with the corresponding four loop perturbative results of [9, 10, 11, 2, 3] provides a nontrivial check on the validity of either approach.

The paper is organised as follows. Section 2 is devoted to introducing background formalism and providing the proof of the critical equivalence of QCD and NATM. In section 3 we develop the large N_f method explicitly in the context of QCD and the NATM. The details of the evaluation of the three loop diagrams to determine the quark anomalous dimension are described at length in section 4. Section 5 is devoted to the development of the Schwinger Dyson formalism to determine the quark anomalous dimension. The computation of the extra three loop graphs needed to determine the mass anomalous dimension is given in section 6. The final results for the quark anomalous dimension and mass anomalous dimension are collected together in section 7 where we also derive new information on the coefficients of the respective RG functions. Several appendices contain results which were fundamental to our calculations.

2 Background.

The QCD Lagrangian in $d = 4 - 2\epsilon$ dimensional Euclidean space reads

$$\mathcal{L} = \bar{\psi}^{iI} \not{D}\psi^{iI} + \frac{1}{4g^2} F_{\mu\nu}^a F^{a\mu\nu} + \frac{1}{2\xi g^2} (\partial \cdot A)^2 + \partial_\mu \bar{c}^a (D^\mu c)^a, \quad (2.1)$$

where ψ^{iI} is the quark field belonging to the fundamental representation of the colour group, $1 \leq I \leq N_f$, A_μ^a is the gluon field, c^a and \bar{c}^a are the ghost fields in the adjoint representation of the colour group, ξ is the covariant gauge parameter and g is the coupling constant. The field strength tensor $F_{\mu\nu}^a$ and the covariant derivative are defined by

$$F_{\mu\nu}^a = \partial_\mu A_\nu^a - \partial_\nu A_\mu^a + f^{abc} A_\mu^b A_\nu^c$$

and

$$D_\mu = (\partial_\mu - iA_\mu^a T^a),$$

where T^a are the colour group generators in the corresponding representation and f^{abc} are the structure constants with $[T^a, T^b] = i f^{abc} T^c$. To ensure the coupling constant, g , is dimensionless below four dimensions we rescale it in the standard way by setting $g \rightarrow M^\epsilon g$, where the parameter M has dimensions of mass. The partition functions of QCD are defined as

$$\langle O_1(x_1) \dots O_n(x_n) \rangle = Z^{-1} \int D\Phi O_1(x_1) \dots O_n(x_n) \exp \{-S\}, \quad (2.2)$$

where $\Phi \equiv \{A, \bar{\psi}, \psi, \bar{c}, c\}$ is the set of fundamental fields, $O_i(x_i)$ represent a basic field or a composite operator and Z is a normalizing factor. As usual, the divergences arising in the calculation of (2.2) are removed by the renormalization procedure at each order of perturbation theory. Namely, provided that the averaging in (2.2) is carried out with the renormalized action all correlators of the fields taken at different space-time points will be finite. The renormalized action $S_R(\Phi, e)$, ($e \equiv \{g, \xi\}$), has the form of the action (2.1) with the fields and parameters being replaced by the bare ones

$$S_R(\Phi, e) = S(\Phi_0, e_0), \quad \Phi_0 = Z_\Phi \Phi, \quad e_0 = Z_e e.$$

Here $Z_\Phi = \{Z_A, Z_\psi, Z_c\}$ and $Z_e = \{Z_g, Z_\xi\}$ are the renormalization constants. However this procedure does not guarantee the finiteness of the Green functions with operator insertions, which contain additional divergences. To remove these extra divergences one should renormalize the composite operators as well. In general, the renormalized operator reads

$$[O_i]_R = \sum_k Z_{ik} O_k, \quad (2.3)$$

where the operators O_k have canonical dimensions equal to or less than those of the original operator O_i , and Z_{ik} is the mixing matrix of renormalization constants. An operator is called multiplicatively renormalized if the matrix Z_{ik} is diagonal, giving $[O_i]_R = Z_i O_i$ where there is no summation over i .

The renormalization group equation (RGE) for the one-particle irreducible n -point Green function with the insertion of k multiplicatively renormalizable composite operators reads

$$\left(M\partial_M + \beta_g \partial_g + \beta_\xi \partial_\xi - n_\Phi \gamma_\Phi + \sum_{i=1}^k \gamma_{O_i} \right) \Gamma(x_1, \dots, x_{n+k}, M, g, \xi) = 0 \quad (2.4)$$

where we use the shorthand notation $n_\Phi \gamma_\Phi = n_A \gamma_A + n_\psi \gamma_\psi + n_c \gamma_c$. The RGE functions β_g , β_ξ , γ_Φ , γ_{O_i} which are the respective beta functions and the anomalous dimensions of the fields and composite operators, are defined as follows

$$\beta_g = M \frac{d}{dM} g(M), \quad \beta_\xi = M \frac{d}{dM} \xi(M), \quad \gamma_\Phi = M \frac{d}{dM} \ln Z_\Phi, \quad \gamma_{O_i} = M \frac{d}{dM} \ln Z_{O_i}. \quad (2.5)$$

Formally, the parameters g and ξ enter (2.4) on the same footing and should be considered as independent charges. However, the gauge fixing parameter ξ is introduced into the theory by hand and cannot enter an expression for a physical quantity. Thus for proper (gauge invariant) objects the term $\beta_\xi \partial_\xi$ drops out of (2.4), which then takes the form of an RGE of a single charge theory.

Our subsequent analysis relies heavily on the existence of a non-trivial infra-red, (IR), stable fixed point g_* of the d -dimensional β -function, $\beta_g(g_*) = 0$, for large values of N_f . The β -function has been calculated in $\overline{\text{MS}}$ using dimensional regularization up to $O(a^6)$ terms, where $a = (g/2\pi)^2 = \alpha_s/\pi$, in [4, 5, 6, 7, 8]. We only record the first few terms here, while the full four loop result can be found in [1],

$$\begin{aligned} \beta_a(a) = & (d-4)a + \left[\frac{2}{3} T_F N_f - \frac{11}{6} C_A \right] a^2 + \left[\frac{1}{2} C_F T_F N_f + \frac{5}{6} C_A T_F N_f - \frac{17}{12} C_A^2 \right] a^3 \\ & - \left[\frac{11}{72} C_F T_F^2 N_f^2 + \frac{79}{432} C_A T_F^2 N_f^2 + \frac{1}{16} C_F^2 T_F N_f - \frac{205}{288} C_F C_A T_F N_f \right. \\ & \left. - \frac{1415}{864} C_A^2 T_F N_f + \frac{2857}{1728} C_A^3 \right] a^4 + O(a^5), \end{aligned} \quad (2.6)$$

from which it follows that

$$a_* = \frac{3\epsilon}{T_F N_f} + \frac{1}{4T_F^2 N_f^2} \left(33C_A \epsilon - [27C_F + 45C_A] \epsilon^2 + O(\epsilon^3) \right) + O\left(\frac{1}{N_f^3}\right). \quad (2.7)$$

The Casimirs for a general classical Lie group are defined by

$$\text{Tr} \left(T^a T^b \right) = T_F \delta^{ab}, \quad T^a T^a = C_F I, \quad f^{acd} f^{bcd} = C_A \delta^{ab}. \quad (2.8)$$

It immediately follows from (2.4) that the Green functions of gauge invariant operators are scale invariant at the critical point g_* . In other words

$$G(\lambda x_i) = \lambda^{D_i} G(x_i),$$

where D_i is the scaling dimension of the corresponding Green function. Moreover, due to the IR nature of the fixed point, this index determines the power of the leading term of the IR asymptotic behaviour of the Green functions ($p_i \rightarrow 0$) near the critical points and this is stable against the perturbation of the action by IR irrelevant operators [25]. On the other hand Green functions of gauge dependent objects, such as the propagators of the basic fields which will in general depend on ξ , are not invariant under scale transformations. Although one may restrict attention from the outset to gauge independent quantities, since they have physical meaning, it is also possible and convenient to choose ξ so that *all* Green functions are scale invariant. Evidently, this is equivalent to the condition $\beta_\xi(g_*, \xi_*) = 0$. Since

$$\beta_\xi(g, \xi) = -2\xi(\epsilon + \gamma_A + \beta_g/g), \quad (2.9)$$

one concludes that the equation $\beta_\xi(g_*, \xi_*) = 0$ has two solutions. One is $\xi_* = 0$ whilst the other is $\gamma_A(g_*, \xi_*) = -\epsilon$. Bearing in mind that our main aim is the development of the $1/N_f$ expansion

we choose the first solution, $\xi = 0$, since the latter gives $\xi \sim N_f$, which leads to problems in the construction of the $1/N_f$ scheme. The origin of the above two solutions for ξ becomes more transparent if one tries to write down the most general form of the gluon propagator satisfying the requirements of both scale and gauge invariance. Indeed, scale invariance yields

$$G_{\mu\nu}(p) = \frac{M^{2\epsilon}}{(p^2)^\alpha} \left(AP_{\mu\nu}^\perp + BP_{\mu\nu}^\parallel \right), \quad (2.10)$$

where $P_{\mu\nu}^\perp$ and $P_{\mu\nu}^\parallel$ are the transverse and longitudinal projectors, respectively, and A and B are constants. As is well known, [25], radiative corrections do not contribute to the longitudinal part of gluon propagator. Hence, $G_{\mu\nu}^\parallel = \xi g^2 M^{2\epsilon} P_{\mu\nu}^\parallel p^{-2}$. This implies, that if $\alpha \neq 1$ then ξ must vanish, $\xi = 0$. On the other hand for $\xi \neq 0$ then one must have $\alpha = 1$ which is easy to check is equivalent to $\gamma_A = -\epsilon$ corresponding to the canonical dimension of the field. Earlier work concerning the relation of scaling and conformal symmetry in the context of gauge theories has been given in [26, 27]. We also note that in an abelian gauge theory the condition $\gamma_A = -\epsilon$ follows directly from the Ward identities that implies the scale invariance of *all* Green functions at the critical point $g = g_*$ in any gauge [24].

As is well known from the theory of the critical phenomena [25] physical systems which look quite different at the microscopic level may exhibit the same behaviour at the phase transition point. An example of this universality is the fixed point relation between the Heisenberg ferromagnet and d -dimensional ϕ^4 field theory. In what follows we construct the theory belonging to the same universality class as large N_f QCD but which has a simpler structure. To this end we develop the $1/N_f$ expansion correlators of the type given in (2.2) and analyse their behaviour in the IR region. As usual, the first step is to integrate over the fermion fields in the functional integral to obtain the effective action for the gluon field

$$S_A^{\text{eff}} \equiv N_f \left(-\text{tr} \ln(\not{\partial} - i\mathcal{A}^a T^a) + \frac{M^{-2\epsilon}}{4\bar{g}^2} (F_{\mu\nu}^a)^2 + \frac{M^{-2\epsilon}}{2\xi\bar{g}^2} (\partial A)^2 \right) + \partial_\mu \bar{c}^a (D^\mu c)^a \quad (2.11)$$

where bearing in mind that $g_*^2 \sim 1/N_f$ we have set $g^2 = \bar{g}^2/N_f$. Assuming that N_f is a large parameter, one can evaluate the integral with action (2.11) by the saddle point method that generates the systematic expansion for the correlators.

We can now examine which terms in (2.11) contribute to the leading IR asymptotics of the correlators. We start our analysis with the gluon propagator in the Landau gauge, $\xi = 0$, which in leading order in $1/N_f$ is

$$G_{\mu\nu}(p) = N_f^{-1} \left[a(p^2)^{d/2-1} + \frac{M^{-2\epsilon}}{2\bar{g}^2} p^2 \right]^{-1} P_{\mu\nu}^\perp = N_f^{-1} a(p^2)^{1-d/2} \left[1 + \frac{1}{2a\bar{g}^2} \left(\frac{p^2}{M^2} \right)^\epsilon \right]^{-1} P_{\mu\nu}^\perp. \quad (2.12)$$

Since $2\epsilon = 4 - d > 0$ the contribution to the propagator from the second term in the brackets of (2.11), $(F_{\mu\nu}^a)^2$, is suppressed by $(p/M)^{2\epsilon}$ in the IR region as compared with the contribution from the fermion loop which is the first term in the brackets. Thus the asymptotic form of the gluon propagator in the IR limit is fully determined by the fermion loop contribution

$$G_{\mu\nu}(p) \stackrel{IR}{\simeq} \frac{a}{N_f} (p^2)^{1-d/2} P_{\mu\nu}^\perp. \quad (2.13)$$

Careful analysis shows that diagrams with triple and quartic gluon vertices do not contribute to the leading IR asymptotics of the correlators either. To see this we note at first that the term $(F_{\mu\nu}^a)^2$ in the action (2.11) may be considered as an ultraviolet regulator with M playing the role of a cutoff. Indeed, due to this term the gluon propagator decreases as $1/p^2$ as $p \rightarrow \infty$, which

makes all diagrams convergent. We note that the appearance of divergences of the type A_μ^2 is prohibited by gauge invariance. Next, if we let G denote an arbitrary diagram, then rescaling the variables in the momentum integrals, $l_i \rightarrow M l'_i$, one finds that up to some prefactor $M^{k\epsilon}$, the parameter M enters the integrand together with the external momenta only. In other words $G(q_{ext}, M) = M^{k\epsilon} G(q_{ext}/M)$. Therefore the limit $q_{ext} \rightarrow 0$ corresponds to the limit $M \rightarrow \infty$, which can be regarded as the removal of the regularization. Further, since the most IR singular contributions we are interested in come from the integration over the region where $l'_i \sim 0$, one can replace the gluon propagator by its asymptotic form (2.13). Then it can be easily checked by simple dimensional analysis that the leading IR singularities come from the diagrams without gluon self-interaction vertices. On the formal level this follows from the fact that term $(F_{\mu\nu}^a)^2$ is accompanied by the factor $M^{-2\epsilon}$ and vanishes in the $M \rightarrow \infty$ limit. So one concludes that this term does not influence the critical properties of the theory and according to the general scheme [25] should be excluded from the action. Therefore we obtain the theory defined by the action

$$S_{NATM} = \bar{\psi}(\not{\partial} - i\not{A}^a T^a)\psi + \frac{N_f}{2\xi}(\square^{-\epsilon/2} \partial A)^2 + \partial_\mu \bar{c}^a \partial^\mu c^a + f^{abc} \partial^\mu \bar{c}^a A_\mu^b c^c, \quad (2.14)$$

which in the Landau gauge has the same critical behaviour as QCD to all orders in the $1/N_f$ expansion. Of course, for gauge independent quantities it is true in any gauge. We have adapted the usual form of the gauge fixing condition to ensure that the transverse and longitudinal parts of the gluon propagator have the same momentum dependence. It is interesting to note that in order to arrive at (2.14) one can start from the theory with manifest gauge invariance which is determined by the action $S = \bar{\psi}(\not{\partial} - i\not{A}^a T^a)\psi$ with ghost and gauge fixing terms in turn arising from the application of the Faddeev-Popov procedure to the functional integral.

Power counting shows that the theory (2.14) is renormalizable within the $1/N_f$ expansion and the renormalized action has the form

$$S_R = Z_1 \bar{\psi} \not{\partial} \psi - i Z_2 \bar{\psi} \not{A}^a T^a \psi + \frac{N_f}{2\xi}(\square^{-\epsilon/2} \partial A)^2 + Z_3 \partial_\mu \bar{c}^a \partial^\mu c^a + Z_4 f^{abc} \partial^\mu \bar{c}^a A_\mu^b c^c \quad (2.15)$$

where we assume, of course, that a gauge invariant regularization is used. Due to the Slavnov-Taylor identities the renormalization constants Z_i are related by

$$Z_2 Z_1^{-1} = Z_4 Z_3^{-1}. \quad (2.16)$$

This equation was used in the exponent formulation to determine the ghost anomalous dimension at $O(1/N_f)$ in the Landau gauge in [15]. As was proved above in the Landau gauge, the critical properties of QCD and this new theory which we shall refer to as the non-abelian Thirring model, (NATM), are identical. Therefore one can use the NATM to deduce the QCD RG functions. This equivalence at leading order in $1/N_f$ was noted in [18] and used to deduce various exponents at $O(1/N_f)$ in [22, 28, 23, 24, 17, 15]. The extension of these calculations to $O(1/N_f^2)$ requires special care. The main one is the necessity of using a gauge invariant regularization which was not crucial at $O(1/N_f)$. The conventional dimensional regularization is not applicable here, since the gluon propagator behaves as $(p^2)^{1-d/2}$ and the theory remains logarithmically divergent in any dimension d . To our knowledge most other invariant regularizations such as higher derivatives spoil the masslessness of the propagators, which makes higher order calculations virtually impossible. Usually in $1/N$ calculations the analytical regularization of [12] is used. However, this breaks gauge invariance.

We now consider how to reconcile gauge invariance with the calculational advantage of using massless propagators. First, we break the gauge invariance of (2.14) from the beginning by introducing a new coupling, λ , for the ghost-gluon vertex of (2.14). For $\lambda = 1$ we recover the

original model but the theory remains renormalizable for arbitrary λ as well. The only effect will be that the identity (2.16) will no longer hold. The bare coupling λ_0 is related to the renormalized one, λ , by

$$\lambda_0 = Z_\lambda \lambda = Z_4 Z_1 Z_2^{-1} Z_3^{-1} \lambda, \quad (2.17)$$

where the Z_i will now also depend on λ . Let us suppose that we used an invariant method, such as regularization by higher derivatives [29], to regularize this extended theory. Then it immediately follows from (2.16) and (2.17) that the equality $\lambda = 1$ for the renormalized coupling implies that $\lambda_0 = 1$ as well. Therefore we conclude that $\lambda = 1$ is a fixed point, $\beta_\lambda(1) = 0$. The existence of this fixed point is the key point and it does not depend on the regularization used. So using any other regularization can only change the position of the fixed point with in general $\lambda_* = 1 + O(1/N_f)$. What is important, though, is that the anomalous dimensions calculated at the critical point, $\gamma(\lambda_*)$, are scheme independent and, hence, coincide with the anomalous dimensions deduced in the original model (2.14). Therefore one can use the regularization which is most convenient from the computational point of view. Moreover, since we do not need to consider diagrams with external ghost legs, then the only diagrams depending on λ are those with a ghost loop. As is evident from counting powers of $1/N_f$ these are themselves $O(1/N_f^2)$. So at this order it is sufficient to set $\lambda = 1$.

3 Methods.

As was shown above the RG functions of QCD at the critical points can be deduced from the more simple NATM. The use of the Δ -regularization [12, 14] allows us to retain massless propagators which means that the calculation of the higher order Feynman integrals can be achieved. However, the price to be paid for this is the loss of the property of multiplicative renormalizability. Indeed, formally, the regularized action has the form

$$\begin{aligned} S_\Delta = & \bar{\psi} \not{\partial} \psi - i \bar{\psi} \not{A}^a T^a \psi + \frac{N_f}{2\xi M^{2\Delta}} \left(\square^{-(\epsilon-\Delta)/2} \partial^\mu A_\mu^a \right)^2 + \partial_\mu \bar{c}^a \partial^\mu c^a + \lambda f^{abc} \partial^\mu \bar{c}^a A_\mu^b c^c \\ & - \frac{1}{2} A_\mu^a(x) M^{-2\Delta} K_\Delta^{\mu\nu}(x, y) A_\nu^a(y) + \frac{1}{2} A_\mu^a(x) K^{\mu\nu}(x, y) A_\nu^a(y). \end{aligned} \quad (3.1)$$

We use $K^{\mu\nu}(x, y) = K^{\mu\nu}(x - y)$ for the inverse fermion loop in coordinate space with

$$(K^{\mu\nu}(x))^{-1} = - \frac{n\Gamma^2(\mu)}{4\pi^{2\mu} |x^{2\mu-1}} \left(g^{\mu\nu} - \frac{2x^\mu x^\nu}{x^2} \right), \quad (3.2)$$

where $n = N_f T_F \text{Tr}_{\text{spinor}} I$. The regularized kernel $K_\Delta^{\mu\nu}(x, y)$ is defined by

$$K_\Delta^{\mu\nu}(x) = C(\Delta) K^{\mu\nu}(x) |x|^{2\Delta} \quad (3.3)$$

and the constant $C(\Delta) = 1 + O(\Delta)$ will be specified below. The last term in (3.1) forms part of the interaction, while the penultimate one is assigned to the free part of the action. Since the last two terms in the action (3.1) are non-local, they are not renormalized and therefore the full renormalized action takes form

$$\begin{aligned} S_\Delta^R = & Z_1 \bar{\psi} \not{\partial} \psi - i Z_2 \bar{\psi} \not{A}^a T^a \psi + \frac{N_f}{2\xi M^{2\Delta}} \left(\square^{-(\epsilon-\Delta)/2} \partial^\mu A_\mu^a \right)^2 + Z_3 \partial_\mu \bar{c}^a \partial^\mu c^a \\ & + Z_4 \lambda f^{abc} \partial^\mu \bar{c}^a A_\mu^b c^c - \frac{1}{2} A_\mu^a(x) M^{-2\Delta} K_\Delta^{\mu\nu}(x, y) A_\nu^a(y) + \frac{1}{2} A_\mu^a(x) K^{\mu\nu}(x, y) A_\nu^a(y). \end{aligned} \quad (3.4)$$

Obviously, S_{Δ}^R cannot be brought into the form (3.1) by the redefinition of the fields and constants. Consequently, the theory with action (3.1) is not multiplicatively renormalizable. A more detailed discussion of this topic can be found in the [14, 30]. The absence of multiplicative renormalizability means the following. We recall that in multiplicatively renormalizable theories the Green functions calculated within two different subtraction schemes are related to each other as follows

$$G_n^I(x_1, \dots, x_n, g) = A_n G_n^{II}(x_1, \dots, x_n, Z_g g) ,$$

where the coefficient $A_n = Z_{\Phi}^n$ and Z_{Φ} is the field renormalization constant. In the case under consideration this equality holds as well. However, $A_n \neq Z_{\Phi}^n$ any longer with A_n depending on n in a nontrivial way. This of course does not contradict the statement about the IR equivalence with QCD, since the IR asymptotics remains unchanged. Nevertheless, the absence of multiplicative renormalizability prevents us from using the standard method of RG analysis for the determination of critical exponents. The more widely used method for this is the method of self-consistency equations, which is based on the direct solution of the Schwinger-Dyson (SD) equations, [12, 14, 22, 28]. Another approach has been developed recently in [20, 21] and will be briefly discussed below in the context of QCD.

3.1 Extended model.

The convenience of the RG method from the computational point of view consists of the possibility of calculating critical exponents via the renormalization constants given in (2.5). To retain this calculational advantage, following the lines of [14, 20, 21], we restore the multiplicative renormalizability of the model in question by attaching two additional charges, u and v , to the last two terms of the action (3.1). Namely, we consider the model with the action

$$S_{uv} = S_{NATM} - \frac{u}{2} A_{\mu}^a(x) M^{-2\Delta} K_{\Delta}^{\mu\nu}(x, y) A_{\nu}^a(y) + \frac{v}{2} A_{\mu}^a(x) K^{\mu\nu}(x, y) A_{\nu}^a(y) . \quad (3.5)$$

Obviously, the initial model (3.1) is recovered by the special choice of the parameters $u = v = 1$.

Figure 1: The effective gluon propagator for $u, v \neq 1$.

As distinct from the initial model the propagator of the gluon field in the model (3.5) with u and v couplings has a more complicated form. Indeed, at $v \neq 1$ the last term in the action (3.5) does not ensure the exact cancellation of the simple fermion loop insertion in the gluon line and one should sum up all such insertions (see figure 1), that yield for the transverse part of the gluon propagator

$$G^{\perp}(p; u, v) \equiv \frac{1}{u} G^{\perp}(p) \left(1 + \frac{(v-1)}{u} t^{\Delta} + \frac{(v-1)^2}{u^2} t^{2\Delta} + \dots \right) , \quad (3.6)$$

with $t \equiv C(\Delta)(M^2/p^2)$. This theory is obviously renormalized. In addition to the standard renormalization constants, Z_1, \dots, Z_4 , which depend now on the couplings u and v , one should add two new ones Z_u and Z_v to take account of the renormalization of the couplings u and v ,

$$u_0 = u M^{-2\Delta} Z_u, \quad v_0 = v Z_v, \quad Z_u = Z_v = Z_A^{-2} .$$

Being multiplicatively renormalizable this model can be analysed with standard RG methods. In particular the basic RG functions are

$$\begin{aligned}\gamma_\Phi &= M\partial_M \ln Z_\Phi, \quad \beta_u = M\partial_M u = 2u(\Delta - \gamma_A), \quad \beta_v = M\partial_M v = -2v\gamma_A, \\ \beta_\xi &= M\partial_M \xi = -2\xi(\Delta - \gamma_A), \quad \beta_\lambda = M\partial_M \lambda,\end{aligned}\quad (3.7)$$

and

$$Z_\psi = Z_1^{1/2}, \quad Z_c = Z_3^{1/2}, \quad Z_A = Z_2 Z_1^{-1}, \quad Z_\lambda = Z_4 Z_3^{-1} Z_1 Z_2^{-1}, \quad Z_\xi = Z_A^2. \quad (3.8)$$

Before discussing the question of the relation of the RG functions of the extended model to the critical exponents of QCD, we derive a compact expression for the RG functions at the point $u = v = 1$. Henceforth we will adopt the minimal subtraction (MS) scheme in which the general renormalization constants have the form

$$Z = 1 + \sum_{n=0}^{\infty} \frac{1}{\Delta^n} Z^{(n)}(u, v, \xi, \lambda).$$

Then taking into account the finiteness of the RG functions and using (3.7) one obtains

$$\gamma = M\partial_M \ln Z|_{u=v=1} = 2(u\partial_u - \xi\partial_\xi)Z^{(1)}(u, v, \xi, \lambda)|_{u=v=1}. \quad (3.9)$$

Since there are no derivatives with respect to λ and v , we can set $\lambda = \lambda_* = 1 + O(1/N_f)$ and $v = 1$ from the very beginning. In this case only the first term in (3.6) survives and, therefore, the operation $(u\partial_u - \xi\partial_\xi)$ applied to a diagram gives simply the number of the gluon lines, n_A , in the latter

$$(u\partial_u - \xi\partial_\xi)\Gamma(u, v, \xi, \lambda)|_{u=v=1} = -n_A \Gamma(1, 1, \xi, \lambda). \quad (3.10)$$

The formula (3.9) can be rewritten as follows

$$\gamma = -2 \sum_{\Gamma} n_A^{(\Gamma)} Z_{\Gamma}^{(1)}(1, 1, \xi, \lambda), \quad (3.11)$$

where the sum runs over the set of all diagrams. Thus to calculate the RG functions defined by (3.9) one can put $u = v = 1$ from the very beginning but take into account the number of gluon lines in each individual graph. To represent (3.11) in a compact form we attach the factor g to the gluon propagator

$$G_{\mu\nu} \rightarrow gG_{\mu\nu}, \quad (3.12)$$

so that each diagram with k internal gluon lines acquires a factor g^k . Then for the anomalous dimensions of the basic fields, (3.9) takes the form

$$\gamma_\Phi = -2g\partial_g Z_\Phi^{(1)}\Big|_{g=1}, \quad (3.13)$$

where the renormalization constants Z_Φ are calculated within the model with $u = v = 1$ and the modified gluon propagator (3.12).

Similarly, the matrix of anomalous dimensions of a system of composite operators, $\{O_i\}$, which mix under renormalization, is given by

$$\gamma_{ik} = 2g\partial_g Z_{ik}^{(1)}\Big|_{g=1} + \delta_{ik} n_{k,\Phi} \gamma_\Phi, \quad (3.14)$$

where the mixing matrix, Z_{ik} , is defined in the standard way from the condition for the Green functions of the renormalized operators O_i^R ,

$$O_i^R = Z_{ik} O_k, \quad (3.15)$$

to be finite. Again, $Z_{ik}^{(1)}$ is the coefficient of the simple pole in Δ . One can easily note the obvious resemblance of the formulæ (3.13) and (3.14) with those used in the MS scheme in dimensional regularization. Therefore using this approach gives a simple and transparent way to compute the critical exponents of operators and, importantly, all the machinery of ϵ expansions can be adapted for the case in question as well.

3.2 Critical exponents and RG functions.

In the previous subsection we have developed the effective tool for the computation of the RG functions $\gamma_{RG} = \gamma_{RG}(u, v)|_{u=v=1}$ in the NATM. The non-trivial exercise is to show that these RG functions, coincide with the corresponding critical exponents γ_{crit} , which determine the scaling properties of the correlators. Generally speaking, this is not so and $\gamma_{RG} \neq \gamma_{crit}$. Indeed, the RG equation for 1-irreducible n -point Green functions with an operator insertion in the extended uv model reads

$$\left([M\partial_M + \beta_U\partial_U + \beta_\xi\partial_\xi + \beta_\lambda\partial_\lambda - n_\Phi\gamma_\Phi]\delta^{ik} + \gamma_{RG}^{ik}\right)\Gamma_k(p_1, \dots, p_{n+1}; u, v, \xi, \lambda) = 0. \quad (3.16)$$

Bearing in mind the critical equivalence between QCD and the NATM in the Landau gauge, we set $\xi = 0$ and $\lambda = \lambda_*$ and do not display their explicit dependence in the Green functions. Since $\beta_\xi(0) = \beta_\lambda(\lambda_*) = 0$ from (3.7), the above equation takes the form

$$\left([M\partial_M + \beta_U\partial_U - n_\Phi\gamma_\Phi]\delta^{ik} + \gamma_{RG}^{ik}\right)\Gamma_k(p_1, \dots, p_{n+1}; u, v, \xi, \lambda) = 0. \quad (3.17)$$

Evidently, due to the presence of the term $\beta_U\partial_U$ in (3.17) the latter does not describe the scaling properties of the Green function $\Gamma_k(p_1, \dots, p_{n+1}; u, v)$ under scale transformation even at the point $u = v = 1$. To make this more transparent, taking into account (3.7), we rewrite (3.17) as follows

$$\left([M\partial_M - n_\Phi\gamma_\Phi]\delta^{ik} + \gamma_{RG}^{ik}\right)\Gamma_k(\{p_l\}) = 2\delta^{ik}\gamma_A(\partial_u + \partial_v)\Gamma_k(\{p_l\}; u, v)\Big|_{u=v=1}. \quad (3.18)$$

It is evident that the matrix γ_{RG}^{ik} can be considered as the matrix of the anomalous dimensions only if the right side of (3.18) is equal to zero. However, since in the Landau gauge $\gamma_A \neq 0$ the right side does not vanish identically. This means that knowledge of the matrix γ_{RG}^{ik} alone is not sufficient for the calculation of the critical exponents.

The problem of the relation of the γ_{RG} and γ_{crit} has been analysed in [20, 21] where it had been shown for the example of the $O(N)$ nonlinear sigma model that the difference $\gamma_{RG} - \gamma_{crit}$ is $O(1/N^3)$. Thus, up to $O(1/N^2)$ the formulæ (3.13) and (3.14) give the true answer for the critical exponents. To prove this statement one has to show that the right side of (3.18) is $O(1/N^3)$. Since the anomalous dimension of the gluon field is $O(1/N_f)$, it is sufficient to prove that the quantity $(\partial_u + \partial_v)\Gamma_k(\{p_l\}; u, v)\Big|_{u=v=1}$ vanishes at $O(1/N_f)$ for any Green function. The proof given in [20] is reduced to the problem of checking this property and without any change can be simply adapted to the present model. More details can be found in [20, 21]. Thus we have justified the use of formulæ (3.13) and (3.14) for the computation of critical exponents in the NATM or QCD in the Landau gauge up to $O(1/N_f^2)$.

It is worth considering what happens in other gauges. Of course, as has been stressed earlier, in this case it is only sensible to consider the anomalous dimensions of gauge invariant operators. In general, the anomalous dimensions of gauge invariant operators, such as $\bar{\psi}\psi$ or $(F_{\mu\nu}^a)^2$, calculated with (3.13) and (3.14) in the extended model, will be gauge dependent. Indeed, we broke the gauge invariance of the model explicitly by introducing the coupling λ

for the ghost-gluon vertex and implicitly by the regularization we have introduced. So it is not surprising that the correlators of gauge invariant objects in this model appear to be gauge dependent. However, it follows immediately from the critical equivalence of QCD and the NATM that at the critical point $\lambda = \lambda_*$ all dependence on ξ in the correlators of gauge invariant operators factorizes

$$\Gamma(x_i, \xi) = A_\Gamma(\xi) \tilde{\Gamma}(x_i), \quad (3.19)$$

where $\tilde{\Gamma}(x_i)$ is already independent of ξ . Then the RG equation for the correlator of two gauge invariant operators $O_1(x)$ and $O_2(y)$ can be cast in the form

$$\left(M\partial_M + \gamma_{O_1} + \gamma_{O_2} + \gamma^* \right) \tilde{\Gamma}(x, y) = 0, \quad (3.20)$$

where $\gamma^* = \beta_\xi \partial_\xi \ln A(\xi)$. Bearing in mind that the explicit breaking of gauge invariance occurs at $O(1/N_f)$ only, ($\lambda_* = 1 + O(1/N_f)$), one can deduce that γ^* is $O(1/N_f^3)$. This immediately leads us to the conclusion that up to $O(1/N_f^2)$ the RG functions of the gauge invariant operator given by the formulæ (3.13) and (3.14) do not depend on the gauge fixing parameter.

Finally, since β_u and β_v as well as β_ξ are proportional to γ_A from (3.7), one can nullify all these beta functions simultaneously choosing the value of the gauge fixing parameter from the condition

$$\gamma_A(\xi_A) = 0, \quad \xi_A = -\frac{(2\mu - 1)}{(\mu - 1)} + O\left(\frac{1}{N_f}\right). \quad (3.21)$$

In this gauge the RG equation in the extended uv model takes the desired form

$$\left([M\partial_M - n_\Phi \gamma_\Phi] \delta_{ik} + \gamma_{RG}^{ik} \right) \Gamma_k(\{p_l\}) = 0, \quad (3.22)$$

from which it follows that the RG functions γ_{RG} are the genuine anomalous dimensions γ_{crit} .

We conclude this section by summarizing the main results:

- In the Landau gauge the critical exponents of QCD at the critical point can be calculated with standard RG methods via the renormalization constants in the extended NATM with the help of the formulæ (3.13) and (3.14) up to $O(1/N_f^2)$.
- Up to $O(1/N_f^2)$ the correspondence between the critical exponents of gauge invariant operators in QCD and NATM holds in any gauge.
- For the special value of the gauge fixing parameter $\xi = \xi_A$ the formulæ (3.13) and (3.14) yield the anomalous dimensions of the gauge invariant operators in *all orders* of $1/N_f$ expansion.

In the next sections we will demonstrate the effectiveness of the above approach by calculating the anomalous dimensions of the quark field and the mass operator $\bar{\psi}\psi$ at second order in the $1/N_f$ expansion. The explicit values of the renormalization constants Z_i and the basic RG functions at $O(1/N_f)$ are given in appendix B.

4 Calculation of graphs.

In this section we discuss the technical details of the calculation of the diagrams relevant for the determination of the anomalous quark dimension. The technique for the evaluation of massless Feynman diagrams is widely documented. (See, for example, [13, 31]). Nevertheless,

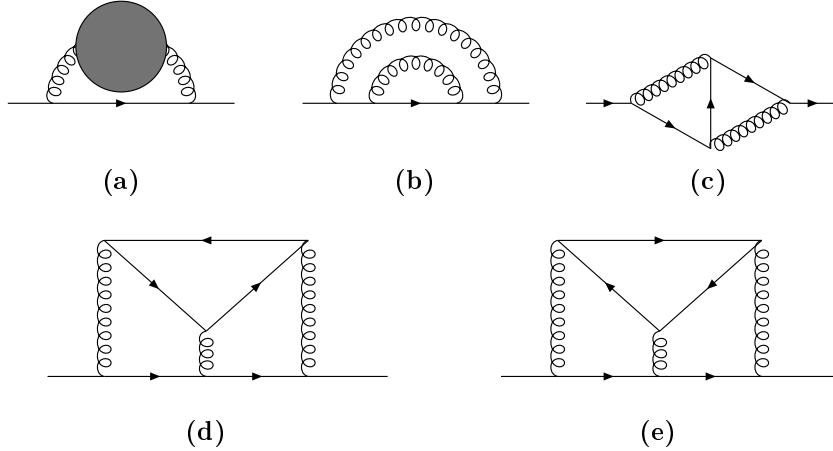


Figure 2: Diagrams contributing to the computation of η_2 . The first graph represents the gluon self energy diagrams of figure 4.

for completeness, we provide a list of basic formulæ, such as the rules for the integration of chains of propagators for scalar, spinor and vector fields and the uniqueness relation for the different type of vertices in appendix A. In what follows we shall concentrate mainly on the calculational problems specific to the case under consideration.

First, we consider the diagrams with external quark legs which are illustrated in figure 2. It transpires that these are not as complicated to evaluate as may appear at first sight. Indeed diagrams (a) and (b) are trivial in that they are equivalent to simple chain graphs in the language of [12]. Although (c) has been considered in the case of QED we re-evaluate it here in the context of the method used to determine diagrams (d) and (e) where the latter differ from each other by a colour factor.

First, for (c) and (d) it is convenient to choose the flow of the external momentum p in both diagrams to be along the fermion line connecting the external vertices. The diagrams are linearly divergent. Differentiating them with respect to the external momentum p_μ one obtains a set of logarithmically divergent diagrams, which differ from the initial ones by the insertion of a new vertex ($-\gamma_\mu$) in each fermion line. This is due to the result

$$\frac{\partial}{\partial p^\mu} \frac{\not{p} + \not{q}}{(p+q)^2} = - \frac{\not{p} + \not{q}}{(p+q)^2} \gamma_\mu \frac{\not{p} + \not{q}}{(p+q)^2}. \quad (4.1)$$

We recall that after subtraction of the divergent subgraphs, in other words after the application of the \mathcal{R}' operation, the residues of the poles in Δ in the diagrams do not depend on the external momenta. Therefore, we are free to choose an arbitrary route for the flow of the external momenta in the each of the resulting diagrams to simplify the subsequent calculations. Our choice is the following. For diagram (c) with the insertion of the vertex ($-\gamma_\mu$) in the vertical fermion line we direct the external momenta flow from the upper to the bottom vertices. When the insertion is in the right or left fermion line we choose the route of the external momenta flow from this new vertex to be along the fermion line nearest to the incoming (outgoing) vertex. After this rearrangement all diagrams are easily integrated since they are reduced to simple chains. For diagram (d) we choose the inserted vertex adjacent to the external one as the new external vertex, and direct the momentum along the fermion line connecting them. Then, the resulting diagram is also reduced to chains but with the insertion of the two loop master diagram in one of the lines, see figure 3. The evaluation of this two loop diagram is straightforward.

We now turn to the discussion on the calculation of the diagrams contributing to the gluon self-energy. These are shown in figure 4 where (b), (c) and the graph involving ghosts, (d),

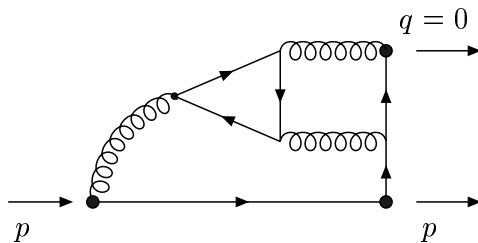


Figure 3: New external momenta routing for the diagram Fig. 4, (d).

are again trivial to determine and do not deserve further comment. On the contrary graphs (a), (e) and (f) are tougher to evaluate and we give details of their determination. As (e) and (f) are related by the same up to the colour factor we will focus on the former. Again (a) was evaluated in the QED calculation but we reconsider it here due to the fact that new techniques were required to evaluate (e) which can more easily be appreciated in a two loop topology. We recall first the standard method for calculating the diagrams with these

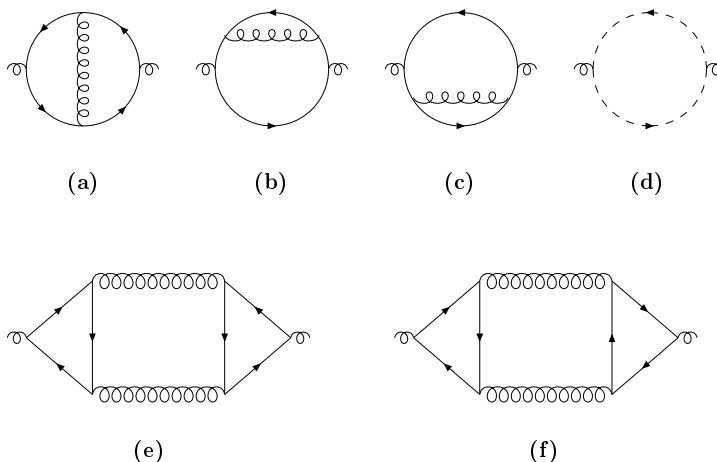
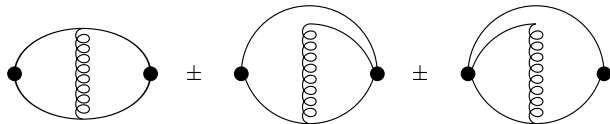


Figure 4: The diagrams contributing to the gluon self-energy at $O(1/N_f^2)$.

topologies in the example of the nonlinear σ model, [12]. It will allow us to avoid the unnecessary complications related to the nontrivial γ -matrix structure of these diagrams in the case of QCD. So, we first consider diagram (a) of figure 4, where now all the lines are assumed to be scalar ones, with respective indices $(2 - \Delta)$ and $(\mu - 1)$ for the wavy and arrowed lines. The diagram is superficially convergent but has two divergent subgraphs. If one could set $\Delta = 0$ then the diagram could be easily integrated due to the uniqueness of the 3-point vertex. To determine this diagram it was suggested in [12] to subtract and add diagrams which have the same singularities as the initial one, but which can be explicitly computed.



Since the singularities cancel in the difference one can take the limit $\Delta \rightarrow 0$. Then all diagrams can be calculated due to uniqueness of the 3-point vertex. The extension of this approach to the case of QCD is possible but leads to the certain problems. The first one is the increase in the number of diagrams to be evaluated. In other words five instead of the one for the nonlinear σ -model. The second and more difficult one is that for $\Delta = 0$ the quark-gluon vertex is not unique. Using the terminology of [31] it is one step from uniqueness, which suggests the

application of the integration by parts method. This also increases the number of integrals to be considered. The calculation of diagrams with propagators having nontrivial tensor structure is more involved compared to scalar ones. Therefore it is desirable to try and keep the number of diagrams during a calculation to a minimum. The approach which is the most economical in this sense is likely to be the one advocated in [31]. Again, we explain the idea in the simple example of the σ model. We shift the indices of the upper lines in diagram (a) by an amount ϵ and the lower ones by $-\epsilon$. In other words we set $\mu - 1 \rightarrow \mu - 1 + \epsilon$ in the top lines. It is important to note that here ϵ is a temporary regularization and ought not to be confused with the parameter which is conventionally used as the dimensional regularization in standard perturbative calculations. The analytic expression for such a diagram can now be written as

$$\frac{1}{\Delta} F(\Delta, \epsilon), \quad (4.2)$$

where $F(\Delta, \epsilon)$ is a regular function in the vicinity of the point $\Delta = \epsilon = 0$. What is important is that we have shifted the indices of the lines in such a way that the pole structure of the diagram has remained unchanged. Next, we need to know this diagram up to constant term in Δ at $\epsilon = 0$. Due to the obvious symmetry $\epsilon \rightarrow -\epsilon$ the function F only depends on ϵ^2 , and its expansion near $\Delta = \epsilon = 0$ is

$$F(\Delta, \epsilon) = F_0 + \Delta F_1 + \Delta^2 F_3 + \epsilon^2 F_4 + O(\Delta^3, \Delta \epsilon^2, \epsilon^4). \quad (4.3)$$

Since the first two terms of the expansion we are interested in are independent of ϵ , one is allowed to evaluate the diagram at any value of ϵ . It is convenient to set $\epsilon = \Delta/2$ which results in the uniqueness of the upper vertex and the diagram is immediately integrable. It is worth noting that one has only to calculate a single diagram instead of five. Applying this procedure twice to the diagram with topology (e) one reproduces the known answer [12] with a minimum amount of calculation. For further discussion it will be important that one is able to determine the subsequent, Δ^2 term in the expansion (4.3) as well. Indeed, bearing in mind that the pole term $F(0, \epsilon)/\Delta$ is fully determined by the counterterm diagrams or, equivalently, is given by the application of the \mathcal{R}' operation to the graph in question, one can easily deduce the coefficient F_4 . This in its turn allows us to fix the value of the coefficient F_3 .

It now seems reasonable to apply this idea to the QCD diagrams. However, one obstacle remains in that the quark-gluon vertex is not unique for the choice of exponents we are restricted to. Though when the propagator of the vector fields has the conformal form

$$G_{\mu\nu}^{conf}(x) = \frac{1}{(x^2)^\beta} \left(\eta_{\mu\nu} - \frac{2x_\mu x_\nu}{x^2} \right), \quad (4.4)$$

then the 3-point fermion vector vertex is unique if the sum of the vertex indices, $2\alpha + \beta$, is equal to $d + 1$, where α is the index of the fermion line. For this unique vertex the relation given in appendix A holds. However the propagator of the gluon field does not have a conformal form. Indeed, at first order in the $1/N_f$ expansion in the Landau gauge it reads

$$G_{\mu\nu}(x) = \frac{\tilde{G}}{(x^2)^{1-\Delta}} \left[\eta_{\mu\nu} + \frac{2(1-\Delta)}{(2\mu-3+2\Delta)} \frac{x_\mu x_\nu}{x^2} \right], \quad (4.5)$$

where \tilde{G} is some constant. Of course, bearing in mind that the calculation of the diagrams with a longitudinal gluon propagator is rather trivial one may represent (4.5) in the following form

$$G_{\mu\nu}(x) = A(\mu, \Delta) G_{\mu\nu}^{conf}(x) + B(\mu, \Delta) G_{\mu\nu}^{\parallel}(x), \quad (4.6)$$

where A and B are some constants and $G_{\mu\nu}^{\parallel}(x)$ is purely longitudinal in momentum space. In such a decomposition it is easy to check that the constants A and B are singular as $\Delta \rightarrow 0$,

$A \sim B \sim 1/\Delta$. The reason for this is that when $\Delta = 0$ the conformal propagator (4.4) coincides with the longitudinal one. If these constants were finite then one could calculate the diagram for the conformal and longitudinal part of the propagator separately. The diagrams with longitudinal propagator would be trivial to integrate, whilst for those with a conformal propagator could be evaluated with the methods we discussed earlier. Now, the singularity in the coefficients of A and B lead to additional difficulties. Namely, due to the additional factor $1/\Delta$ in the coefficients A and B one should evaluate this diagram with higher accuracy in Δ . However it is a reasonable price to pay for the considerable simplification which arises from the uniqueness of the triple vertex.

In the following we shall mainly discuss diagram (e) of figure 4 since its evaluation was the most difficult. We will focus our discussion on the more important points as the intermediate steps are not difficult to reproduce. However, to give an impression about the effectiveness of the suggested approach it is instructive to discuss the calculation of the QED type, diagram figure 4(a), first. Using the decomposition (4.6) one reduces the problem to the calculation of the diagram with the conformal propagator (4.4) with index $\gamma = 1 - \Delta$, where the calculation of the diagram with longitudinal propagator is trivial. Due to the singularity of the coefficient $A(\Delta)$ this diagram should be evaluated up to terms linear in Δ . Following the scheme discussed above in the case of the scalar diagram we introduce the additional regularizing parameter $\pm\epsilon$ in the upper and lower lines. Then the analytic expression for this diagram is given by the same formula (4.3), where all the necessary Lorentz indices are implied. For $\epsilon = \Delta/2$ the diagram can be integrated due to the uniqueness of the upper vertex, while the coefficient F_4 , as was explained earlier, can be extracted from the one loop counterterm diagrams. Thus, we have reduced the determination of the photon self energy diagram to the calculation of four chains.

We now consider the calculation of the three loop gluon self energy diagram. First, since

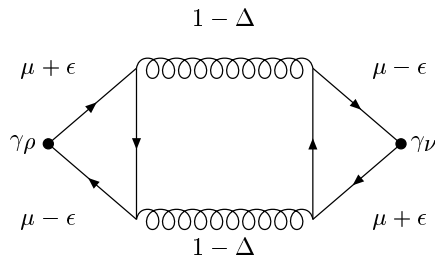


Figure 5: Three loop gluon self energy diagram with ϵ and Δ regularizations.

the longitudinal part of the gluon polarization tensor $\Pi_{\rho\nu}(p)$ can be easily calculated, it is sufficient to calculate the above diagram with contracted indices, Π_ν^ν , which simplifies the algebra significantly. Moreover, the contributions of all the diagrams in figure 4 to the longitudinal part of the gluon polarization cancel identically. Further, since the calculation of the diagram with the longitudinal propagator is trivial, we shall discuss only those with the conformal ones. For this diagram we again introduce the additional regularization ϵ in the fermion lines as shown in figure 5. The diagram, being superficially convergent with two divergent two loop subgraphs, the analytic expression for it is given as follows

$$\Pi(\Delta, \epsilon) = \frac{1}{\Delta} \left(\Pi_0 + \Delta\Pi_1 + \Delta^2\Pi_2 + \Delta^3\Pi_3 + \epsilon^2\Pi_4 + \epsilon^2\Delta\Pi_5 + O(\Delta^4, \Delta^2\epsilon^2, \epsilon^4) \right). \quad (4.7)$$

We recall that our purpose is to determine the function $\Pi(\Delta, 0)$ up to the Δ^3 terms. In other words we are interested in the coefficients Π_0 , Π_1 , Π_2 and Π_3 .

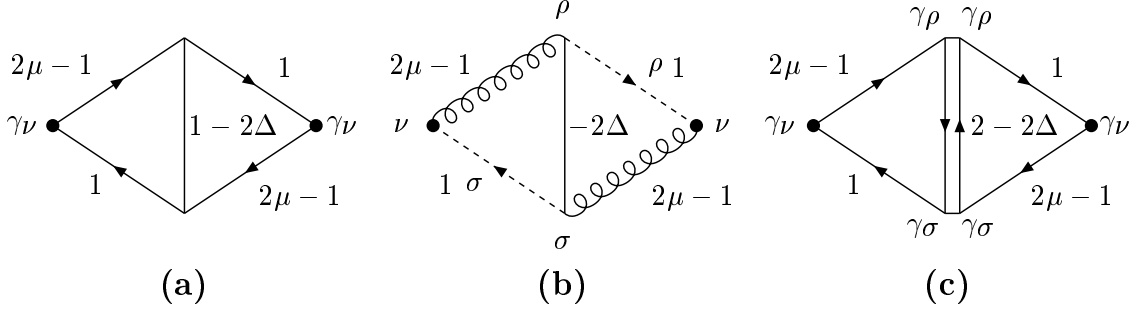


Figure 6: The three resulting diagrams for $G^{conf} \otimes G^{conf}$ case.

The strategy of the calculation is the following. For $\epsilon = \Delta$ one can exploit the uniqueness of the lower right and upper left vertices to evaluate the diagram, which allows us to find the coefficients Π_0 and Π_1 and the combination of coefficients $\Pi_2 + \Pi_4$ and $\Pi_3 + \Pi_5$. To extract Π_2 and Π_3 we evaluate the coefficients Π_4 and Π_5 . The former is determined by the counterterm diagrams and its calculation is straightforward, while the evaluation of the latter is more nontrivial and will be discussed below. At first, however, we consider in more detail the computation of the diagram for a special value of the parameter ϵ . We take $\epsilon = \Delta$, which restores the uniqueness of the two vertices.

Using the uniqueness relation one can express the initial diagram as the sum of two loop diagrams, which after some algebra can be reduced to the ones shown in figure 6 and a chain integral. Here the wavy line with labels ν and ρ denotes the conformal propagator $G_{\nu\rho}^{conf}$. The dashed line with label ρ and index α is used for the propagator $x_\rho/(x^2)^\alpha$. In diagram (c) the vertical double line is used to represent $\not{x} \otimes \not{x}$ where each \not{x} enters from a different fermion cycle. We discuss briefly the calculation of each of the diagrams shown in figure 6.

- Diagram (a).

This diagram enters the expansion with a coefficient proportional to $\gamma - 1 = -\Delta$ so we need to calculate it up to $O(\Delta)$. To this end we shift the indices of upper fermion line by ϵ , and the lower ones by $-\epsilon$. The analytic structure of this modified diagram is the following

$$\Pi_a(\Delta, \epsilon) = \frac{R(\epsilon)}{\Delta} + R'(\Delta, \epsilon) = \frac{1}{\Delta}(R_0 + \epsilon^2 R_1 + O(\epsilon^4)) + R'_0 + R'_1 \Delta + O(\Delta^2, \epsilon^2), \quad (4.8)$$

where we took into account the fact that due to the $\epsilon \rightarrow -\epsilon$ symmetry the diagram depends on ϵ^2 only. Further, the diagram can be integrated at $\epsilon = \Delta$ due to uniqueness of the Gross-Neveu type at the upper vertex. Again, the coefficient R_1 is determined by the counterterm diagrams and can be easily evaluated. This is sufficient to determine $\Pi_a(\Delta, 0)$ with the required accuracy.

- Diagram (b).

At first we note that this diagram is finite as $\Delta \rightarrow 0$ and we need it up to $O(\Delta^2)$. Again, we shift the indices of the wavy lines by $+\epsilon$ and $-\epsilon$. Then the expansion of this new diagram in Δ and ϵ reads

$$\Pi_b(\Delta, \epsilon) = \Delta R_0 + \Delta^2 R_1 + \epsilon^2 R_2 + \dots \quad (4.9)$$

When $\Delta = 0$ the diagram can be calculated exactly which allows us to find the coefficient R_2 . Next, it can be checked that the diagram can be integrated for $\epsilon = 2\Delta$ as well. Indeed, representing $(\eta_{\nu\rho} - 2x_\nu x_\rho/x^2)(z-x)^\rho$ as

$$z_\nu - x_\nu \frac{z^2}{x^2} + x_\nu \frac{(z-x)^2}{x^2},$$

where we choose the coordinates of the left and right vertices to be 0 and z respectively, and the upper vertex to be x , one obtains three diagrams. The first two of them can be calculated due to the uniqueness of the upper vertex, whilst the last is a simple chain. We note that one needs to introduce an additional regularization δ , by for example shifting the index of the lower dashed line of the original diagram by δ , to make each of the resulting diagrams finite. Of course, the sum of the diagrams is finite in the $\delta \rightarrow 0$ limit. Again it is sufficient to determine $\Pi_b(\Delta, 0)$ with the required accuracy, $\Pi_b(\Delta, 0) = \Pi_b(\Delta, 2\Delta) - \Pi_b(0, 2\Delta)$.

- Diagram (c).

The last diagram enters the expansion with the coefficient $(\gamma - 1)^2 = \Delta^2$. So one needs to calculate it with $O(1)$ accuracy. The calculation runs along the same lines as above. We shift the indices of the upper lines by $+\Delta$, and the lower ones by $-\Delta$, which evidently does not influence the Δ^0 terms. To simplify the γ -matrix structure of the diagrams it is convenient to represent the tensor product of the γ -matrix, $\gamma_\rho \otimes \gamma^\rho$ where each γ -matrix enters from different traces, as $\gamma^\rho \hat{G}_{\rho\lambda} \otimes \hat{G}^{\lambda\rho'} \gamma_{\rho'}$, where x is the coordinate of the upper vertex and $\hat{G}_{\rho\lambda}$ is the numerator of the conformal propagator (4.4). We repeat this exercise for $\gamma_\sigma \otimes \gamma^\sigma$ and $\gamma_\nu \otimes \gamma^\nu$. Then, using the following identities

$$\not{x} \gamma^\rho \hat{G}_{\rho\lambda}(x) = -\gamma_\lambda \not{x}, \quad \hat{G}_{\lambda\sigma}(x) \gamma^\sigma = -\not{x} \gamma_\lambda \not{x} / x^2$$

both traces can be cast into the form suitable for the inversion transformation. After the inversion the upper vertex decouples from the base (left vertex) and the diagram can be immediately integrated.

The evaluation of the coefficient Π_5 is grounded on the following observation. Since in the momentum space representation the conformal propagator takes the form

$$G^{conf}(p) = \frac{\tilde{A}}{(p^2)^{\mu-1+\Delta}} \left(P^\parallel(p) - \frac{\Delta}{2(\mu-1+\Delta)} P^\perp(p) \right) \quad (4.10)$$

the contributions to the $\epsilon^2 \Delta$ term come only from the momentum integral involving two longitudinal propagators $P^\parallel \otimes P^\parallel$, or longitudinal and transverse ones, $P^\parallel \otimes P^\perp$. Moreover, because the transverse propagator enters the expansion (4.10) with an additional factor Δ , the contribution from the latter can be extracted again from the consideration of the counterterm diagrams alone, and does not require much work. Thus the nontrivial part of the calculation is the determination of the diagram in question with the longitudinal propagators. We shall use the momentum representation and at the first step contract one momentum from the numerator of each longitudinal gluon propagators into the fermion traces. After this the initial diagram reduces to four integrals. Two of these are identical whilst another is a simple chain integral. Therefore, we are left with two nontrivial diagrams which are shown in figure 7. For later convenience we replace the regulator ϵ in the right fermionic triangles by δ . We consider the left hand diagram first and denote it by $G(\Delta, \epsilon, \delta)$. We look for the ϵ^2 term in the expansion of function $G(\Delta, \epsilon, \delta)$. It is easy to see that for $\epsilon \rightarrow 0$ with Δ and δ fixed that $G \rightarrow 0$ as well. Indeed in the $\epsilon \rightarrow 0$ limit the left hand triangle turns into a fermion loop, which is transverse, so that when it is contracted with the incoming momenta it vanishes. Thus one concludes that $G(\Delta, \epsilon, \delta) = \epsilon \delta \tilde{G}(\Delta, \epsilon, \delta)$ and

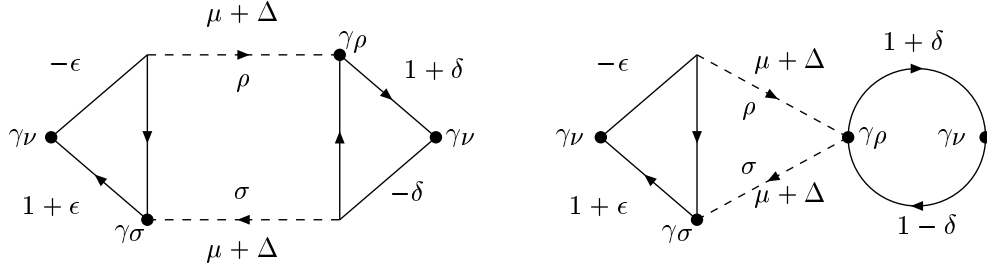


Figure 7: Two diagrams contributing to the evaluation of Π_5 . The indices of lines are given in the momentum space version.

for our purpose it is therefore sufficient to calculate $\epsilon\delta\tilde{G}(0,0,0)$, where we take into account the finiteness of the diagram. This implies the following method for its evaluation. We ascribe the label 1 to the regulators ϵ and δ on the upper fermion lines and replace $\epsilon \rightarrow \epsilon_1$ and $\delta \rightarrow \delta_1$. Similarly for the lower lines we replace ϵ by ϵ_2 and δ by δ_2 there. Hence, the diagram now depends on four variables $G(\epsilon_1, \epsilon_2, \delta_1, \delta_2)$. Then $\epsilon^2\tilde{G}(0,0,0) = G(\epsilon, 0, \epsilon, 0) + G(\epsilon, 0, 0, \epsilon) + G(0, \epsilon, 0, \epsilon, 0) + G(0, \epsilon, 0, \epsilon)$ and each of these four diagrams can be reduced to chain integrals which completes the evaluation of this graph.

The calculation of the right hand diagram of figure 7 is more involved. In momentum space it corresponds to

$$\Pi(\Delta, \epsilon) = \frac{\Pi^{\nu\rho}(\Delta, \epsilon)P_{\nu\rho}^\perp(p)}{(p^2)^{1-\mu+2\Delta}}, \quad (4.11)$$

where the transverse projector arises from the fermion loop and the nontrivial piece, $\Pi_{\nu\rho}$, comes from the two loop master diagram. We begin with the analysis of the analytic structure of the two loop integral. First, it is superficially divergent so one has

$$\Pi_{\nu\rho}(\Delta, \epsilon) = \eta_{\nu\rho} \frac{R(\epsilon)}{\Delta} + \text{regular terms} .$$

Second, for the same reason as we discussed for the previous graph $\Pi_{\nu\rho}(\Delta, \epsilon) \rightarrow 0$ as $\epsilon \rightarrow 0$. Third, the residue at the Δ pole is independent of ϵ . Indeed, since the divergence is logarithmic the residue does not depend on the external momenta. Then, choosing a new route for the external momenta flow, for example along the vertical line, one can see that all the dependence on ϵ disappears. Since $\Pi_{\nu\rho}(\Delta, 0) = 0$, we conclude that $R = 0$ and therefore the diagram is finite. Moreover, it is not hard to check that the terms proportional to $\eta_{\nu\rho}$ are even in ϵ , and therefore we have

$$\Pi_{\nu\rho}(\Delta, \epsilon) = \left[\epsilon^2 \eta_{\nu\rho} A + \frac{p_\nu p_\rho}{p^2} (\epsilon D + \epsilon^2 B + \epsilon \Delta C) \right]. \quad (4.12)$$

For $\epsilon = \Delta$ the diagram with contracted indices can be reduced, in coordinate space, to the sum of chain integrals and one with a unique vertex of the Gross-Neveu type. Next, it can be checked that $g^{\nu\rho}\Pi_{\nu\rho}(\Delta, \Delta) = 0$ which results in the following constraints on the coefficients

$$D = 0, \quad 2\mu A + B + C = 0 .$$

We recall that due to the presence of the transverse projector in (4.11) we are only interested in the coefficient A . However, it is easier to calculate coefficients B and C and find A from the above constraint. To determine C we repeat the technique used for the evaluation of the previous

diagram. In other words we set $\epsilon \rightarrow \epsilon_{1(2)}$ for the upper and lower lines, respectively. Then, C is equal to the coefficient of the $\epsilon\Delta$ term in the sum of the two diagrams $\Pi_{\nu\rho}(\Delta, \epsilon_1 = 0, \epsilon_2 = \epsilon) + \Pi_{\nu\rho}(\Delta, \epsilon_1 = \epsilon, \epsilon_2 = 0)$, which are easy to integrate. To deduce B we first transform the master diagram into coordinate space, giving

$$\frac{1}{(x^2)^{\mu-2\Delta}} \tilde{\Pi}_{\nu\rho}(x, \Delta, \epsilon) .$$

It is easy to check that for $\Delta = 0$, only the term proportional to B survives in $\tilde{\Pi}$ with $\tilde{\Pi}_{\nu\rho}(x, \Delta, \epsilon) \sim B(\eta_{\nu\rho} - 2\mu x_\nu x_\rho/x^2) + O(\Delta)$. Next, we use tetrahedral symmetry whereby we add the new line, $x_\nu x_\rho/(x^2)^{1+\kappa}$, to the diagram to obtain a vacuum graph. The integration over x yields the pole in κ which is independent of which line we place the regularizing parameter, κ , [33]. Thus we can place the regulator on the vertical line and change the order of integration where we integrate over the upper vertex last. After some algebra the new diagram can be reduced to chains which allows us to determine the coefficient B , and hence the coefficient A which we are interested in.

Clearly, the evaluation of the three loop contribution to the gluon propagator is a tedious exercise. To ensure that we have determined it correctly, aside from the checks we will discuss later, we have also undertaken to calculate it by another method. As this is equally as long an exercise we will briefly summarize the main steps. It is based on the original method of subtractions of [12] but differs from the one outlined above in that the original Feynman diagram is broken up into a sum of scalar integrals by taking spinor traces and the relevant Lorentz projections. Although this results in a large set of integrals the majority of them are in fact reducible to simple chain integrals or graphs involving the two loop self energy master diagram. The latter can readily be evaluated by uniqueness methods. The remaining three loop graphs fall into two classes. Either they are divergent, and therefore their simple pole and finite part with respect to Δ need to be determined, or they are fully Δ -finite. In the former case we were able to apply integration by parts and related methods to again reduce them to integrals which were chains, master diagrams or additionally three loop integrals which were evaluated by subtraction methods to the finite part. The purely Δ -finite integrals, in fact, represented

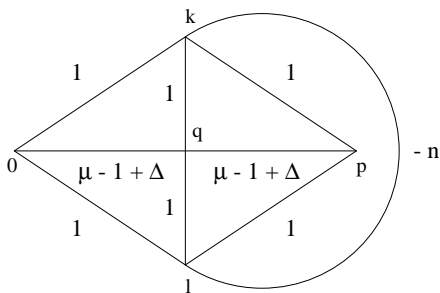


Figure 8: Finite three loop diagrams contributing to gluon self-energy.

the most difficult to determine and were of the form given in figure 8 where $n = 0, 1, 2$ or 3 and k, l and q are the loop momenta with p the external momentum. In this notation the negative integer exponent corresponds to a numerator factor in the integrand, $((k - l)^2)^n$. The $n = 0$ case had been treated previously in [12]. To determine the other graphs we considered a related diagram which involved fermion lines constructed in such a way that when the n traces were computed the original scalar diagram of figure 8 emerged. The additional integrals which accompanied this were again either chains or two loop self energy graphs, aside of course from the new fermionic graph. This was evaluated by applying a Fourier transform to map it to

coordinate space before taking the spinor traces. However, to avoid intermediate singularities in this step which arise from anti-uniqueness we introduced a temporary analytic regularization, δ , in the exponents of the propagators. The advantage of transforming to coordinate space is that the resulting scalar integrals all have a vertex where the scalar uniqueness relation can be applied to leave chain integrals. For completeness we note that the values of the integral of figure 8 are

$$\begin{aligned}
& - \frac{(\mu-1)a^4(1)a^2(2\mu-2)}{2\Gamma(\mu)} \left[\Phi(\mu) + \Psi^2(\mu) + \frac{a^3(1)a(2\mu-3)}{(2\mu-3)(\mu-2)} \right. \\
& \left. + \frac{(4\mu-7)(3\mu-4)\Psi(\mu)}{(2\mu-3)(\mu-2)(\mu-1)} + \frac{(13\mu^2-35\mu+23)}{(2\mu-3)(\mu-1)^2(\mu-2)} \right] \quad (4.13)
\end{aligned}$$

for $n = 2$ and

$$\begin{aligned}
& \frac{a^4(1)a^2(2\mu-2)}{2(2\mu-1)\Gamma(\mu)} \left[\mu(\mu-1) \left(\Phi(\mu) + \Psi^2(\mu) \right) - \frac{\mu(\mu-1)a^3(1)a(2\mu-3)}{(2\mu-1)(2\mu-3)(\mu-2)} \right. \\
& \quad + \frac{3(12\mu^4-48\mu^3+63\mu^2-30\mu+4)\Psi(\mu)}{(2\mu-1)(2\mu-3)(\mu-2)} \\
& \quad \left. + \frac{(58\mu^5-232\mu^4+339\mu^3-230\mu^2+78\mu-12)}{(2\mu-1)(2\mu-3)(\mu-1)(\mu-2)\mu} \right] \quad (4.14)
\end{aligned}$$

for $n = 3$. Including these with the other values we have verified that the same value for the three loop gluon self energy is obtained in the Landau gauge.

This completes our detailed discussion of the evaluation of the three loop self energy diagrams and we now collect all the contributions and record the final values for all the relevant Feynman diagrams. First, we consider the gluon polarization tensor. To fix normalization we write down the expressions for the propagators in momentum space

$$G_\psi = \frac{i\not{p}}{p^2}, \quad G_{gh} = \frac{1}{p^2}, \quad G_{\nu\rho} = \frac{G M^{2\Delta}}{n(p^2)^{\mu-1+\Delta}} \left[\eta_{\nu\rho} - (1-\xi) \frac{p_\nu p_\rho}{p^2} \right],$$

where the amplitude G in the gluon propagator reads

$$G = \frac{(4\pi)^\mu \Gamma(2\mu)}{2\Gamma^2(\mu)\Gamma(2-\mu)}. \quad (4.15)$$

Further, the contribution from the i -th graph of figure 4 to the polarization tensor $\Pi_{\mu\nu}$ can be written in momentum space as

$$\Pi_{\mu\nu}^{ab,i}(p) = \frac{\delta^{ab}}{(p^2)^{1-\mu+n_i\Delta}} \left(A^i P_{\mu\nu}^\perp + B^i P_{\mu\nu}^\parallel \right), \quad \Pi_{\mu\nu} = \sum_i \Pi_{\mu\nu}^i. \quad (4.16)$$

Here P^\perp, P^\parallel are the transverse and longitudinal projectors and n_i is the number of the gluon lines in the diagram. The calculation yields for the coefficients B^i

$$\begin{aligned}
B^a &= - (C_F - C_A/2) R_1, & B^{b+c} &= C_F R_1, \\
B^d &= C_A R_2, & B^{e+f} &= - C_A (R_1 + R_2), \quad (4.17)
\end{aligned}$$

where

$$\begin{aligned}
R_1 &= \frac{(2\mu-1)(\mu-2)}{(4\pi)^\mu \mu(\mu-1)\Gamma(\mu)} \left[1 + \frac{\xi\mu}{(2\mu-1)(\mu-2)} \right], \\
R_2 &= - \frac{\Gamma^2(\mu)a(2\mu-1)}{2(4\pi)^\mu}. \quad (4.18)
\end{aligned}$$

As can be seen they are all finite and their sum vanishes, $\sum_i B^i = 0$.

Instead of recording the values for A^i we list the values for the coefficients Π^i , which are related to the former as

$$A^i = \frac{\Pi^i - B^i}{(2\mu - 1)},$$

and, as is easy to see, they are given by the trace of the corresponding contributions to the polarization tensor, $\Pi^i = \Pi^i_{\nu}{}^{\nu}$. We find

$$\begin{aligned} \Pi^a &= 2 \left(C_F - \frac{C_A}{2} \right) R(\Delta) \times \\ &\times \left[\frac{1}{\Delta} \left(1 + \frac{\xi\mu}{(\mu-2)(2\mu-1)} \right) - \frac{3\mu(\mu-1)}{(\mu-2)(2\mu-1)} \left(\Theta(\mu) - \frac{1}{(\mu-1)^2} \right) \right], \end{aligned} \quad (4.19)$$

$$\Pi^b = \Pi^c = -C_F R(\Delta) \left[\frac{1}{\Delta} \left(1 + \frac{\xi\mu}{(\mu-2)(2\mu-1)} \right) + \frac{2(\mu-1)}{\mu(\mu-2)} \right], \quad (4.20)$$

$$\Pi^d = -\frac{C_A}{(4\pi)^\mu} \Gamma^2(\mu) a(2\mu-1), \quad (4.21)$$

$$\begin{aligned} \Pi^{ef} &= C_A \frac{R(2\Delta)}{2} \left(\frac{\mu-1}{\mu-2} \right) \left[\frac{1}{\Delta} \left(1 + \frac{\xi}{\mu-1} \right) - \frac{2\mu\Gamma^3(\mu)a(2\mu-1)}{(\mu-1)(2\mu-1)^2} \right. \\ &+ \frac{2\mu}{(2\mu-1)} \left(\Psi^2(\mu) + \Phi(\mu) - 6\Theta(\mu) \right) - \frac{\mu(8\mu^4 - 76\mu^3 + 198\mu^2 - 193\mu + 62)}{(2\mu-1)^2(2\mu-3)(\mu-1)(\mu-2)} \Psi(\mu) \\ &+ \frac{2(8\mu^7 - 60\mu^6 + 206\mu^5 - 374\mu^4 + 346\mu^3 - 149\mu^2 + 34\mu - 6)}{(2\mu-1)^2(2\mu-3)(\mu-1)^2(\mu-2)\mu} \\ &\left. - \frac{2\xi\Psi(\mu)}{(2\mu-1)} - \frac{\xi(10\mu^4 - 34\mu^3 + 27\mu^2 + 10\mu - 12)}{\mu(\mu-1)^2(\mu-2)(2\mu-1)(2\mu-3)} - \frac{\xi^2\mu}{2(\mu-1)^2(2\mu-1)} \right]. \end{aligned} \quad (4.22)$$

Here

$$R(\Delta) = -\frac{(\mu-2)(2\mu-1)^2 a(\mu-1+\Delta)a(1-\mu)}{(4\pi)^\mu \mu(\mu-1+\Delta)a(1-\mu+\Delta)},$$

and the functions $\Psi(\mu)$, $\Phi(\mu)$ and $\Theta(\mu)$ are defined as

$$\begin{aligned} \Psi(\mu) &= \psi(2\mu-3) + \psi(3-\mu) - \psi(1) - \psi(\mu-1), \\ \Phi(\mu) &= \psi'(2\mu-3) - \psi'(3-\mu) - \psi'(\mu-1) + \psi'(1), \\ \Theta(\mu) &= \psi'(\mu-1) - \psi'(1), \end{aligned} \quad (4.23)$$

where $\psi(x) = (\ln \Gamma(x))'$. Taking into account (4.16) the renormalized gluon propagator is

$$G_{\nu\rho}(p) = \frac{G}{n(p^2)^{\mu-1}} \left[\left(1 + \frac{1}{n} \left[r + \gamma_A^{(1)} \ln(p^2/M^2) \right] \right) P_{\nu\rho}^\perp + \xi P_{\nu\rho}^\parallel \right], \quad (4.24)$$

where

$$\gamma_A^{(1)} = -\sum_i n_i \Pi_{-1}^{(i)} = \frac{C_A \eta_0}{2(\mu-2)} \left(1 + \frac{\xi(\mu-1)}{(2\mu-1)} \right), \quad (4.25)$$

$$r = \sum_i \Pi_0^{(i)} = \frac{\eta_0}{2(\mu-2)} \left[C_F \left(\frac{6\mu(\mu-1)}{(2\mu-1)} \left(\Theta(\mu) - \frac{1}{(\mu-1)^2} \right) + \frac{4(\mu-1)}{\mu} \right) \right]$$

$$\begin{aligned}
& + \frac{C_A}{(2\mu-1)} \left(-\mu(\mu-1) \left(\Psi^2(\mu) + \Phi(\mu) - 3\Theta(\mu) \right) \right. \\
& + \frac{(8\mu^5 - 92\mu^4 + 270\mu^3 - 301\mu^2 + 124\mu - 12)\Psi(\mu)}{2(\mu-2)(2\mu-1)(2\mu-3)} \\
& - \frac{(16\mu^7 - 120\mu^6 + 420\mu^5 - 776\mu^4 + 742\mu^3 - 349\mu^2 + 84\mu - 12)}{2\mu(\mu-1)(\mu-2)(2\mu-1)(2\mu-3)} \\
& \left. + \frac{\xi}{2} \left(\frac{(\mu^2 + 2\mu - 2)}{\mu(\mu-1)} + \frac{\xi\mu}{2(\mu-1)} \right) \right) \Bigg] , \tag{4.26}
\end{aligned}$$

and the functions $\Pi_0^{(i)}$ and $\Pi_{-1}^{(i)}$ are defined as

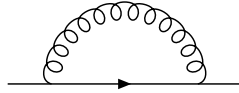
$$\Pi^{(i)} = \eta_0 (2\mu-1) G^{-1} \left[\frac{\Pi_{-1}^{(i)}}{\Delta} + \Pi_0^{(i)} \right] . \tag{4.27}$$

Finally, η_0 is twice the anomalous quark dimension in Landau gauge which is recorded in (B.3),

$$\eta_0 = \frac{(\mu-2)(2\mu-1)\Gamma(2\mu)}{\Gamma^2(\mu)\Gamma(\mu+1)\Gamma(2-\mu)} . \tag{4.28}$$

We note that the part of the polarization tensor corresponding to the QED contribution is independent of the gauge fixing parameter ξ which is consistent with a general analysis. For example, see [25].

Next we turn to the quark propagator and record the values for the graphs of figure 2. First, for completeness we write down the value for the graph



which contributes to the fermion propagator at $O(1/N_f)$. Straightforward calculations give

$$i\not{p} \left(\frac{4M^2}{p^2} \right)^\Delta \frac{C_F\eta_0}{2\Delta} \left[1 + \frac{\xi\mu}{(2\mu-1)(\mu-2)} + \frac{2(\mu-1)\Delta}{\mu(\mu-1)} + O(\Delta^2) \right] \tag{4.29}$$

for the above graph which results in the following anomalous quark dimension at $O(1/N_f)$

$$\gamma_\psi^{(1)} = \frac{C_F\eta_0}{2} \left(1 + \frac{\xi\mu}{(2\mu-1)(\mu-2)} \right) \tag{4.30}$$

and the renormalized propagator

$$G_\psi(p) = \frac{i\not{p}}{p^2} \left[1 + \frac{C_F}{n} \left(-\frac{(\mu-1)\eta_0}{\mu(\mu-2)} + \gamma_q^{(1)} \ln(p^2/M^2) \right) \right] . \tag{4.31}$$

Here and elsewhere we use the notation $A = \sum_k A^{(k)}/n^k$.

Below we list the \mathcal{KR}' values of the graphs of figure 2, which are necessary to determine the quark anomalous dimension at $O(1/N_f^2)$. The value of each graph after application of the \mathcal{KR}' operation will be denoted by the respective capital letter. So, for example, applying \mathcal{KR}'

to graph (b) of 2 gives $i\not{p}B$. In addition $A^{(i)}$ corresponds to the value of the i -th subgraph of figure 4. We find

$$A^{(i)} = C_F \eta_0 \left[\frac{(n_i - 2)}{2n_i \Delta^2} \Pi_{-1}^{(i)} + \frac{1}{2n_i \Delta} \left(\Pi_0^{(i)} - \frac{B^{(i)}}{(2\mu - 1)} \left(1 - \frac{\xi\mu}{(\mu - 2)} \right) \right) \right], \quad (4.32)$$

$$B = \frac{C_F^2 \eta_0^2}{8} \left(1 + \frac{\xi\mu}{(\mu - 2)(2\mu - 1)} \right)^2 \left[\frac{1}{\Delta^2} - \frac{1}{\Delta\mu} \right], \quad (4.33)$$

$$C = -C_F \left(C_F - \frac{C_A}{2} \right) \frac{\eta_0^2}{4} \times \left[\left(\frac{1}{\Delta^2} - \frac{1}{2\Delta\mu} \right) \left(1 + \frac{\xi\mu}{(\mu - 2)(2\mu - 1)} \right)^2 + \frac{2(\mu - 1)(\mu^2 - \mu - 1)}{\mu(\mu - 2)^2(2\mu - 1)\Delta} \right], \quad (4.34)$$

$$D + E = -\frac{C_A \eta_0^2}{12} \left[\frac{(\mu - 1 + \xi)[(\mu - 2)(2\mu - 1) + \xi\mu]}{(\mu - 2)^2(2\mu - 1)\Delta^2} + \frac{3\mu(\mu - 1)}{(\mu - 2)(2\mu - 1)\Delta} \Theta(\mu) - \frac{4\mu^4 - 10\mu^3 + 9\mu^2 + 4\mu - 2}{2\mu(\mu - 1)(\mu - 2)(2\mu - 1)\Delta} \right] \quad (4.35)$$

$$+ \frac{\xi(\mu^2 - 4\mu + 2)}{\mu(\mu - 2)^2(\mu - 1)(2\mu - 1)\Delta} \left(1 + \frac{\xi\mu}{2} \right) \Big]. \quad (4.36)$$

According to (3.13) the anomalous quark dimension at $O(1/N_f^2)$ is given by the sum of the residues at simple poles in Δ multiplied by the number of gluon lines in the diagrams. The final result for η_2 will be given in section 7.

5 Schwinger Dyson approach.

In this section we present the Schwinger Dyson, (SD), formalism to determine the exponent η_2 . There are various motivations for this. One is that in the context of the newer approach of the previous sections it will allow an interested reader to compare and contrast the technology involved. Though in fact it will not represent a significant amount of extra work given that the difficult Feynman integrals have now been evaluated. Second, it provides another check on our calculations as it is clear these are quite technical. Third, we would like to discuss some distinctions in the treatment of the theories with abelian and nonabelian gauge symmetries in the SD approach. Our first comment concerns the issue of choosing the gauge fixing parameter, ξ , entering the gluon propagator. To appreciate the subtlety of this choice we recall that in the original construction of Vasil'ev et al for scale invariant theories, such as ϕ^4 theory, [12], one omits at the outset the contribution of the bare propagator in the SD equation, which is less singular in the infra-red region compared to the loop corrections. This converts the SD equations into self-consistency equations which determine the exponents of the propagators. In respect of the discussion of the previous sections concerning QCD and the NATM, scale invariance is only present in two gauges. These are the Landau gauge, $\xi = 0$, and that given by $\xi = \xi_A$ in (3.21). Therefore, strictly speaking, our subsequent SD analysis will only be valid for these particular gauges. By contrast in an abelian gauge theory such as QED the gauge propagator is scale invariant in any gauge in the $1/N_f$ expansion. To understand how the choice of these two gauges arises from demanding scale invariance one can repeat the arguments given in section 2. Indeed, on general grounds the form of the full gluon propagator in the massless limit will take the form

$$\tilde{A}_{\mu\nu}(k) = \frac{\tilde{B}^\perp}{(k^2)^{\mu-\beta}} \left[\eta_{\mu\nu} - \frac{k_\mu k_\nu}{k^2} \right] + \tilde{B}^\parallel \xi \frac{k_\mu k_\nu}{(k^2)^\mu}. \quad (5.1)$$

Clearly to have a scale invariant gluon propagator the exponents of the momentum prefactor in the transverse and longitudinal pieces both ought to be the same. This can come about in two ways subject to the physical restriction of retaining the transverse part. One case is to have no longitudinal part which gives rise to the Landau gauge, $\xi = 0$. The other is to match the powers of the exponents in each term. This requires the gluon to have zero anomalous dimension, $\eta + \chi = 0$. Since this exponent is gauge dependent then one can in principle solve this equation order by order in large N_f perturbation theory to determine the explicit value of ξ . It is this solution which we denote by ξ_A . It is worth noting that in QED, [22, 23], the photon anomalous dimension vanishes in all gauges by virtue of the QED Ward identity and therefore the ansatz for the photon propagator was automatically scale invariant. Alternatively another point of view can be taken on this problem. One can solve the SD equations in a nonabelian gauge theory taking a scale invariant ansatz for the gluon propagator with an arbitrary gauge fixing parameter. This parameter is then considered as an input parameter which is to be determined. Therefore, it is not hard to understand that solving the SD equations one will find that the latter are only consistent for two particular values of ξ . These will be $\xi = 0$ and $\xi = \xi_A$.

In light of these observations we now proceed with the SD calculation but restrict ourselves to the Landau gauge. Therefore, the ansatz for the gluon propagator in this calculation is,

$$\tilde{A}_{\mu\nu}(k) = \frac{\tilde{B}}{(k^2)^{\mu-\beta}} \left[\eta_{\mu\nu} - \frac{k_\mu k_\nu}{k^2} \right] \quad (5.2)$$

in momentum space. The gluon propagator exponent is given by

$$\beta = 1 - \eta - \chi \quad (5.3)$$

where χ is the quark gluon vertex anomalous dimension. For the quark and ghost fields we define their momentum space propagators as

$$\tilde{\psi}(k) = \frac{\tilde{A}k}{(k^2)^{\mu-\alpha}} \quad , \quad \tilde{c}(k) = \frac{\tilde{C}}{(k^2)^{\mu-\gamma}} \quad (5.4)$$

where \tilde{A} , \tilde{B} and \tilde{C} are the momentum independent amplitudes. The analogous coordinate space amplitudes will be A , B and C respectively. In the SD critical point method, [12], one determines the unknown exponent, η , by representing the two point SD equations at the appropriate order which is $O(1/N_f^2)$. The representation of the equations form a set of algebraic equations with various unknowns one of which is η whilst the others are combinations of the amplitudes \tilde{A} , \tilde{B} and \tilde{C} . Eliminating the latter variables allows one to deduce η .

The figure shows the quark Schwinger-Dyson equation at order $O(1/N_f^2)$. It is represented as an equation: $0 = \psi^{-1} +$ followed by three diagrams separated by plus signs. The first diagram is a quark line with a gluon loop (a wavy line forming a circle). The second diagram is a quark line with a ghost loop (a wavy line forming a circle). The third diagram is a quark line with a ghost loop and a ghost-gluon loop (a wavy line forming a circle with a smaller wavy line inside it).

Figure 9: Quark Schwinger Dyson equation to $O(1/N_f^2)$.

To illustrate these points we focus initially on the quark equation as there are additional features which need to be considered in the treatment of the gluon equation which will be discussed later. If we denote by Σ_1 and Σ_2 the values of the respective two and three loop graphs of figure 9 in coordinate space then the SD equation at $O(1/N_f^2)$ can be represented

algebraically by

$$0 = r(\alpha - 1) + \Sigma_0 z m^2 (x^2)^{\chi + \Delta} + C_F (C_F - C_A/2) (x^2)^{2\chi + 2\Delta} z^2 \Sigma_1 + C_F C_A (x^2)^{3\chi + 3\Delta} T_F N_f z^3 \Sigma_2 \quad (5.5)$$

where

$$\Sigma_0 = 2 \left[\frac{(\beta - \Delta)}{(2\mu - 2\beta - 1 + 2\Delta)} - (\mu - 1) \right], \quad (5.6)$$

corresponds to the first graph of figure 9 and $z = A^2 B$. The analytic regularization has been included by shifting the vertex anomalous dimension from χ to $\chi + \Delta$. As in the original method of [12] we have chosen the coordinate space representation of the Schwinger Dyson equation. To relate to the momentum space version one applies the usual Fourier transform

$$\frac{1}{(x^2)^\alpha} = \frac{a(\alpha)}{2^{2\alpha} \pi^\mu} \int_k \frac{e^{ikx}}{(k^2)^{\mu - \alpha}} \quad (5.7)$$

to the version of (5.5) prior to the powers of x^2 being cancelled. The coordinate space propagators can be determined from (5.2) and (5.4) and are taken to be

$$\begin{aligned} \psi(x) &= \frac{A \not{x}}{(x^2)^\alpha}, \quad A_{\mu\nu}(x) = \frac{B}{(x^2)^\beta} \left[\eta_{\mu\nu} + \frac{2\beta}{(2\mu - 2\beta - 1)} \frac{x_\mu x_\nu}{x^2} \right] \\ c(x) &= \frac{C}{(x^2)^\gamma}. \end{aligned} \quad (5.8)$$

The inverse quark propagator, which is the origin of the first term of (5.5), is given by

$$\psi^{-1}(x) = \frac{r(\alpha - 1) \not{x}}{A (x^2)^{2\mu - 2\alpha + 1}} \quad (5.9)$$

where

$$r(\alpha) = \frac{\alpha a(\alpha - \mu)}{\pi^{2\mu} (\mu - \alpha) a(\alpha)}. \quad (5.10)$$

In (5.5) the quantity m corresponds to the vertex renormalization constant which will absorb the divergences arising in the two and three loop corrections. To make this more explicit we define their Δ -dependence as

$$\Sigma_i = \frac{K_i}{\Delta} + \Sigma'_i \quad (5.11)$$

where the $O(\Delta)$ terms are not important at this order in $1/N_f$. Therefore the quark Dyson equation is rendered finite by defining the counterterm formally as

$$m_1 = \frac{(2\mu - 3)z_1}{4(2\mu - 1)(\mu - 2)T_F} [(C_F - C_A/2)K_1 + C_A z_1 K_2] \quad (5.12)$$

where we have set

$$m = 1 + \frac{m_1}{N_f \Delta} + O\left(\frac{1}{N_f^2}\right), \quad z = \frac{z_1}{N_f} + \frac{z_2}{N_f^2} + O\left(\frac{1}{N_f^3}\right). \quad (5.13)$$

However, this leaves terms in the SD equation involving $\ln x^2$ which would otherwise spoil the simple scaling behaviour at the fixed point. To avoid this one defines the vertex anomalous dimension to be

$$\chi_1 = \frac{(2\mu - 3)z_1}{2(2\mu - 1)(\mu - 2)T_F} [(C_F - C_A/2)K_1 + 2C_A z_1 K_2]. \quad (5.14)$$

With these definitions the finite quark Dyson equation to $O(1/N_f^2)$ is

$$0 = r(\alpha - 1) + C_F \left[\frac{\Sigma_{00} z_1}{N_f} + \frac{(\Sigma_{00} z_2 + \Sigma_{02} z_1 + 2m_1 \Sigma_{01} z_1)}{N_f^2} \right] \\ + C_F (C_F - C_A/2) \frac{z_1^2}{N_f^2} \Sigma'_1 + C_F C_A \frac{z_1^3}{N_f^2} \Sigma'_2 \quad (5.15)$$

where the first term contains η_1 and η_2 and we have expanded Σ_0 as

$$\Sigma_0 = \Sigma_{00} + \Delta \Sigma_{01} + \frac{(\Sigma_{02} + \Delta \Sigma_{03})}{N_f} + O\left(\frac{1}{N_f^2}; \Delta^2\right). \quad (5.16)$$

Therefore, from (5.15) we can determine a relation for η_2 in terms of z_2 and the finite correction graphs, as

$$\eta_2 = \frac{z_2 \eta_1}{z_1} + \frac{\eta_1^2}{2\mu} + \left[\Sigma_{02} + 2m_1 \Sigma_{01} + (C_F - C_A/2) z_1 \Sigma'_1 + C_A z_1^2 \Sigma'_2 \right] \frac{\eta_1}{\Sigma_{00}} \quad (5.17)$$

where $\eta = \sum_{i=1}^{\infty} \eta_i / N_f^i$ and $\eta_1 = \gamma^{(1)} / (2T_F)$ in earlier notation.

For the gluon SD equation there is the added complication of dealing with the transverse and longitudinal components of the equation. Whilst this has been dealt with for QED in [23] we will recall the important features. In coordinate space the inverse gluon propagator is, [32, 23],

$$A_{\mu\nu}^{-1}(x) = \frac{m(\beta)}{B(x^2)^{2\mu-\beta}} \left[\eta_{\mu\nu} + \frac{2(2\mu - \beta)}{(2\beta - 2\mu - 1)} \frac{x_\mu x_\nu}{x^2} \right] \quad (5.18)$$

where

$$m(\beta) = \frac{(2\mu - 2\beta + 1)(2\mu - 2\beta - 1)a(\beta - \mu)}{4\pi^{2\mu}(\mu - \beta)^2 a(\beta)}. \quad (5.19)$$

We recall, [32, 23], that this is deduced by inverting the gauge dependent momentum space gluon propagator on the physical transverse subspace before Fourier transforming back to coordinate space. Therefore, we can formally represent the coordinate gluon SD equation as

$$0 = m(\beta - \Delta) \left[\eta_{\mu\nu} + \frac{2(2\mu - \beta + \Delta)}{(2\beta - 2\mu - 1 - 2\Delta)} \frac{x_\mu x_\nu}{x^2} \right] - 4zT_F N_f m^2(x^2)^{\chi+\Delta} \left[\eta_{\mu\nu} - \frac{2x_\mu x_\nu}{x^2} \right] \\ - (C_F - C_A/2) T_F N_f z^2 (x^2)^{2\chi+2\Delta} \left[\eta_{\mu\nu} \Pi_1 + \frac{x_\mu x_\nu}{x^2} \Xi_1 \right] \\ + C_A T_F^2 N_f^2 z^3 (x^2)^{3\chi+3\Delta} \left[\eta_{\mu\nu} \Pi_2 + \frac{x_\mu x_\nu}{x^2} \Xi_2 \right] \\ - \frac{C_A \gamma^2 (2\mu - 2\beta - 1) a^2(\mu - \gamma) (x^2)^{\chi_c + \Delta} \tilde{y} x^\mu x^\nu}{2(\mu - \beta) a(\beta) x^2} \quad (5.20)$$

where Π_1 and Ξ_1 relate to the coordinate space value of the two loop diagram of figure 10 and Π_2 and Ξ_2 correspond to that of the three loop one. The final term of (5.20) is the ghost contribution from the ghost graph of figure 10. However, its treatment requires special care. Although we have constructed the gluon equation in coordinate space, the ghost contribution is determined from its evaluation in momentum space since the ghost couples via a derivative to the gluon. This explains the appearance of the amplitude combination $\tilde{y} = \tilde{C}^2 \tilde{B}$ in (5.20). In particular the ghost graph of figure 10 is

$$- C_A \nu(\mu - \gamma, \mu - \gamma, 2\gamma + 1) \frac{\gamma^2 \tilde{C}^2}{2(2\gamma + 1)(p^2)^{\mu-2\gamma-1}} \left[\eta^{\mu\nu} + 2(2\gamma - \mu + 1) \frac{p^\mu p^\nu}{p^2} \right]. \quad (5.21)$$

$$\begin{aligned}
0 &= A_{\mu\nu}^{-1} + \text{[Diagram 1]} + \text{[Diagram 2]} \\
&+ \text{[Diagram 3]} + \text{[Diagram 4]}
\end{aligned}$$

Figure 10: Gluon Schwinger Dyson equation to $O(1/N_f^2)$.

Although the ghost was treated in large N_f in the Landau gauge in [15] where its anomalous dimension and vertex anomalous dimension were computed at $O(1/N_f)$, the value of \tilde{y}_1 was not recorded. To determine it we consider the ghost SD equation of figure 11. In momentum space it becomes

$$0 = 1 + (2\mu - 1)\tilde{y}C_A \frac{\nu(\mu - \gamma - 1, \mu - \beta, \beta + \gamma)}{2(\mu - \gamma - 1)(\beta + \gamma)(\mu - \beta)} \quad (5.22)$$

whence

$$\tilde{y}_1 = - \frac{\mu\Gamma(\mu)\eta_{c,1}}{(2\mu - 1)C_A} \quad (5.23)$$

where $\eta_c = \sum_{i=1}^{\infty} \eta_{c,i}/N_f^i$. Alternatively using the Slavnov-Taylor identity in the Landau gauge we have

$$\tilde{y}_1 = \frac{\Gamma(\mu + 1)\eta_0}{2(\mu - 2)(2\mu - 1)T_F}. \quad (5.24)$$

We note that in (5.20) the x -dependence of the final term involves χ_c . This emerges after using the Slavnov-Taylor identity in rationalising powers of x^2 in the initial representation of the SD equation.

Whilst there appears to be two components of (5.20) to analyse it turns out that only one is important. This is the transverse component when expressed in momentum space using the Fourier transform. Although this may appear to neglect information contained in the longitudinal part of the equation with respect to momentum space it turns out in fact that the sum of contributions to the longitudinal projection of (5.20) in momentum space from the various graphs in arbitrary gauge is actually zero. The cancellation in the C_F sector was discussed in [23]. For the C_A sector the contributions from the longitudinal sectors of the last three graphs of figure 10 sum to zero which can be verified from the explicit values of the graphs. This is also true for non-zero ξ .

Therefore, returning to (5.20) and restoring the common factor of $1/(x^2)^{2\mu-\beta+\Delta}$ in each term we transform the equation to momentum and retain only the transverse part. Inverting this component to coordinate space yields the relevant part of the gluon SD equation for determining

$$0 = c^{-1} + \text{[Diagram 5]}$$

Figure 11: Ghost Schwinger Dyson equation at $O(1/N_f)$.

the critical exponents,

$$\begin{aligned}
0 &= \frac{2(\mu - \beta + \Delta)m(\beta - \Delta)}{(2\mu - 2\beta + 1 + 2\Delta)} - \frac{8(\alpha - 1)zT_F N_f m^2(x^2)^{\chi + \Delta}}{(2\alpha - 1)} \\
&\quad - (C_F - C_A/2)T_F N_f z^2(x^2)^{2\chi + 2\Delta} \left[\Pi_1 + \frac{\Xi_1}{2(2\alpha - 1 - \chi - \Delta)} \right] \\
&\quad + C_A T_F^2 N_f^2 z^3(x^2)^{3\chi + 3\Delta} \left[\Pi_2 + \frac{\Xi_2}{2(2\alpha - 1 - 2\chi - 2\Delta)} \right] \\
&\quad - \frac{C_A \gamma^2 (2\mu - 2\beta - 1) a^2 (\mu - \gamma) (x^2)^{\chi_c + \Delta} \tilde{y}}{4(2\gamma + 1)(\mu - \beta)a(\beta)}
\end{aligned} \tag{5.25}$$

which now requires renormalization. This is performed in the same way that (5.5) was rendered finite. Repeating the procedure here and ensuring that there is no anomalous scaling behaviour we find,

$$\begin{aligned}
0 &= \frac{2(\mu - \beta)m(\beta)}{(2\mu - 2\beta + 1)} - \frac{8(\alpha - 1)zT_F N_f}{(2\alpha - 1)} \\
&\quad - (C_F - C_A/2)T_F N_f z^2 \left[\Pi'_1 + \frac{\Xi'_1}{2(2\alpha - 1)} + \frac{X_1}{2(2\alpha - 1)^2} \right] \\
&\quad + C_A T_F^2 N_f^2 z^3 \left[\Pi'_2 + \frac{\Xi'_2}{2(2\alpha - 1)} + \frac{X_2}{(2\alpha - 1)^2} \right] - \frac{C_A \gamma^2 (2\mu - 2\beta - 1) a^2 (\mu - \gamma) \tilde{y}}{4(2\gamma + 1)(\mu - \beta)a(\beta)}
\end{aligned} \tag{5.26}$$

where we have defined

$$\Pi_i = \frac{P_i}{\Delta} + \Pi'_i \quad , \quad \Xi_i = \frac{X_i}{\Delta} + \Xi'_i \tag{5.27}$$

for $i = 1$ and 2 , and

$$\begin{aligned}
m_1 &= -\frac{(2\mu - 1)z_1}{16(\mu - 1)} \left[\left(C_F - \frac{C_A}{2} \right) \left(P_1 + \frac{X_1}{2(2\mu - 1)} \right) - C_A z_1 \left(P_2 + \frac{X_2}{2(2\mu - 1)} \right) \right] \\
\chi_1 &= -\frac{(2\mu - 1)z_1}{8(\mu - 1)} \left[\left(C_F - \frac{C_A}{2} \right) \left(P_1 + \frac{X_1}{2(2\mu - 1)} \right) - 2C_A z_1 \left(P_2 + \frac{X_2}{2(2\mu - 1)} \right) \right] .
\end{aligned} \tag{5.28}$$

Although it may seem that (5.12) and (5.14) will give different values from (5.28), when the explicit values for the residues of the simple poles in Δ are substituted, they are equivalent. Moreover, the value of χ_1 will agree with (5.14). Having made the gluon Schwinger Dyson equation finite, it is elementary to expand (5.26) to $O(1/N_f^2)$ to obtain an expression for z_2 . We find

$$\begin{aligned}
\frac{z_2}{z_1} &= (\eta_1 + \chi_1) \left[\Psi(\mu) + \frac{1}{2(\mu - 1)} + \frac{1}{(\mu - 2)} + \frac{2}{(2\mu - 3)} \right] \\
&\quad - \frac{(2\mu - 1)}{8(\mu - 1)} \left[\frac{4\eta_1}{(2\mu - 1)^2} + C_A \frac{(2\mu - 3)\Gamma(\mu)\tilde{y}_1}{4(2\mu - 1)z_1} \right. \\
&\quad \quad + \left(C_F - \frac{C_A}{2} \right) z_1 \left(\Pi'_1 + \frac{\Xi'_1}{2(2\mu - 1)} + \frac{X_1}{2(2\mu - 1)^2} \right) \\
&\quad \quad \left. - C_A z_1^2 \left(\Pi'_2 + \frac{\Xi'_2}{2(2\mu - 1)} + \frac{X_2}{(2\mu - 1)^2} \right) \right] .
\end{aligned} \tag{5.29}$$

Therefore with this value for z_2 we can establish a formal expression for η_2 in arbitrary gauge which depends only on the values of the various graphs of figures 9, 10 and 11 by eliminating

z_2 in (5.17). For completeness, we quote the coordinate space values of the integrals which will determine η_2 from these equations. First, we recall the graphs of the QED sector are

$$\Sigma_1 = \frac{4}{\mu(2\mu-3)^2\Gamma^2(\mu)} \left[\frac{2(2\mu-1)^2(\mu-2)^2}{\Delta} + 4(\mu-1)^2 \left(\frac{2(\mu-1)^2}{\mu} + \frac{(2\mu-3)}{2} \right) - 4(2\mu-1) - (2\mu-1)(\mu-2) - \frac{8(2\mu-1)^2(\mu-2)^2}{(2\mu-3)} \right] \quad (5.30)$$

$$\Pi_1 = -\frac{\Xi_1}{2} = -\frac{16}{(2\mu-3)\Gamma^2(\mu)} \left[\frac{(2\mu-1)(\mu-2)}{\mu\Delta} + \frac{3}{(\mu-1)} - 3(\mu-1)\Theta(\mu) - \frac{2(2\mu-1)(\mu-2)}{\mu(2\mu-3)} \right]. \quad (5.31)$$

For the three loop graphs we have

$$\Sigma_2 = -\frac{8(2\mu-1)^2(\mu-2)}{(2\mu-3)^3\mu^2\Gamma^4(\mu)\eta_0} \left[\frac{(2\mu-1)(\mu-2)(\mu-1)}{\Delta} - 6\mu(\mu-1)(\mu-2)\Theta(\mu) + [8\mu^6 - 48\mu^5 + 118\mu^4 - 130\mu^3 + 34\mu^2 + 35\mu - 12]/[\mu(\mu-1)(2\mu-3)] \right] \quad (5.32)$$

and

$$\begin{aligned} \Pi_2 = & -\frac{8}{(2\mu-3)^2\mu^2\Gamma^4(\mu)\eta_0} \left[\frac{2(2\mu-1)^2(\mu-1)(\mu-2)}{\Delta} \right. \\ & + 4\mu(2\mu-1)(\mu-1)(\mu-2)[\Phi(\mu) + \Psi^2(\mu) - 6\Theta(\mu)] \\ & - \frac{2\mu\Psi(\mu)}{(2\mu-3)}(8\mu^4 - 76\mu^3 + 198\mu^2 - 193\mu + 62) \\ & + 8(4\mu^7 - 34\mu^6 + 123\mu^5 - 222\mu^4 + 197\mu^3 - 78\mu^2 + 16\mu - 3) \\ & \left. /[\mu(\mu-1)(2\mu-3)] \right]. \quad (5.33) \end{aligned}$$

The longitudinal component is related to Π_2 by

$$\Xi_2 = -2\Pi_2 + \frac{64}{(2\mu-3)^2\mu^2\Gamma^4(\mu)\eta_0} \left[(2\mu-1)(\mu-2) + \frac{\mu(\mu-1)^2\alpha^3(1)}{2(2\mu-3)a(3-\mu)} \right]. \quad (5.34)$$

Therefore, substituting the values of the integrals in the formal expressions for χ_1 and m_1 , we have explicitly

$$m_1 = -\frac{C_F\eta_0}{2T_F} - \frac{(2\mu-1)(\mu-3)C_A\eta_0}{8(2\mu-1)(\mu-2)T_F} \quad (5.35)$$

$$\chi_1 = -\frac{C_F\eta_0}{T_F} - \frac{C_A\eta_0}{2(\mu-2)T_F}. \quad (5.36)$$

The relation between the coordinate space variables and the momentum space ones of earlier sections is determined from the Fourier transform of the asymptotic scaling forms. For instance, it is easy to deduce that the respective quark amplitudes A and \tilde{A} are related by

$$\tilde{A} = -\frac{ia(\alpha-1)A}{(\alpha-1)} \quad (5.37)$$

whilst the respective gluon amplitudes are determined from comparing the coefficients of the $\eta_{\mu\nu}$ component. We find

$$\tilde{B} = \frac{2(\mu-\beta)a(\beta)B}{(2\mu-2\beta-1)}. \quad (5.38)$$

Thus,

$$\tilde{z} = - \frac{(\mu - \beta)a^2(\alpha - 1)a(\beta)z}{(\alpha - 1)^2(2\mu - 2\beta - 1)} \quad (5.39)$$

which implies

$$\tilde{z}_1 = - \frac{2z_1}{(2\mu - 3)\Gamma(\mu)} \quad (5.40)$$

and

$$\tilde{z}_2 = - \frac{2}{(2\mu - 3)\Gamma(\mu)} \left[z_2 - \frac{2z_1\eta_1}{(2\mu - 3)} \right] \quad (5.41)$$

upon expanding in powers of $1/N_f$. Moreover, variables involving the ghost amplitudes are related by $\tilde{y} = a^2(\gamma)a(\beta)y$. Similarly, we can relate the values of the three loop integrals expressed in either coordinate or momentum space. For instance, if the value of the three loop gluonic graph in coordinate space is

$$\frac{1}{(x^2)^{2\mu-1-2\Delta}} \left[\Pi_2 \eta_{\mu\nu} + \Xi_2 \frac{x_\mu x_\nu}{x^2} \right] \quad (5.42)$$

and in momentum space

$$\frac{1}{(p^2)^{1-\mu+2\Delta}} \left[\tilde{\Pi}_2 \eta_{\mu\nu} + \tilde{\Xi}_2 \frac{p_\mu p_\nu}{p^2} \right] \quad (5.43)$$

then we have,

$$\begin{aligned} \Pi_2 &= \frac{4(\mu - 1 + \Delta)^2 a^6 (\mu - 1) a^2 (1 - \Delta)}{(\mu - 1)^6 (2\mu - 3 + 2\Delta)^2 a (2\mu - 1 - 2\Delta)} \left[\tilde{\Pi}_2 - \frac{\tilde{\Xi}_2}{2(\mu - 1 - 2\Delta)} \right] \\ \Xi_2 &= \frac{4(\mu - 1 + \Delta)^2 (2\mu - 1 - 2\Delta) a^6 (\mu - 1) a^2 (1 - \Delta) \tilde{\Xi}_2}{(\mu - 1 - 2\Delta) (\mu - 1)^6 (2\mu - 3 + 2\Delta)^2 a (2\mu - 1 - 2\Delta)}. \end{aligned} \quad (5.44)$$

Likewise,

$$\Sigma_2 = \frac{(\mu - 3\Delta)(\mu - 1 + \Delta)^3 a^5 (\mu - 1) \tilde{\Sigma}_2}{16(\mu - 1)^5 (2\mu - 3 + 2\Delta)^3 a^3 (\mu - 1 + \Delta) a (\mu - 3\Delta)}. \quad (5.45)$$

So, for example, the finite parts of the momentum space integrals are given by

$$\begin{aligned} \tilde{\Pi}'_2 &= \frac{8(\mu - 1)^3 a^4 (1) a^2 (2\mu - 2)}{(2\mu - 1)^2 \Gamma(\mu)} \left[4 \left(\Psi^2(\mu) + \Phi(\mu) - 6\Theta(\mu) \right) \right. \\ &\quad - \frac{a^3(1)}{(2\mu - 1)(2\mu - 3)(\mu - 2)a(3 - \mu)} \\ &\quad + \frac{(32\mu^7 - 176\mu^6 + 524\mu^5 - 952\mu^4 + 927\mu^3 - 468\mu^2 + 180\mu - 48)}{(\mu - 1)^2 (2\mu - 1)(2\mu - 3)(\mu - 2)\mu^2} \\ &\quad \left. - \frac{4}{(\mu - 1)} \left(\Psi(\mu) + \frac{(4\mu^5 - 16\mu^4 + 32\mu^3 - 40\mu^2 + 25\mu - 6)}{(2\mu - 1)(2\mu - 3)(\mu - 1)(\mu - 2)\mu^2} \right) - \frac{1}{(\mu - 1)^2} \right] \end{aligned} \quad (5.46)$$

$$\begin{aligned} \tilde{\Xi}'_2 &= - \tilde{\Pi}'_2 - \frac{8a^4(1)a^2(2\mu - 2)}{(2\mu - 1)^2 \Gamma(\mu)} \left[2(\mu - 1) \right. \\ &\quad \left. - \frac{(\mu - 1)^3}{(2\mu - 3)(\mu - 2)\mu} \left(4(2\mu - 3)(\mu - 2) - \frac{\mu a^3(1)}{a(3 - \mu)} \right) \right] \end{aligned} \quad (5.47)$$

and

$$\tilde{\Sigma}'_2 = \frac{2(\mu - 1)(2\mu - 1)^2(\mu - 2)^2}{\mu^2 \Gamma^3(\mu) \eta_0} \left[\Theta(\mu) - \frac{(4\mu^5 - 6\mu^4 - 13\mu^3 + 40\mu^2 - 40\mu + 10)}{6\mu^2(\mu - 1)^2(\mu - 2)} \right]. \quad (5.48)$$

6 Mass anomalous dimension.

Having presented the formalism to calculate the quark anomalous dimension at $O(1/N_f^2)$ we are now turn to the quark mass anomalous dimension at the same order. Perturbatively the mass anomalous dimension is known to four loop accuracy. Thus comparison of results obtained in both perturbation theory and the $1/N_f$ expansion will provide a non-trivial test on the validity of our results since, for instance, only three loop diagrams are considered at $O(1/N_f^2)$ in the large N_f formalism. To complete the calculation we discuss some observations here which allow us to relate the values of most of the graphs contributing to the mass dimensions at $O(1/N_f^2)$ to those used for the quark anomalous dimensions. It transpires that this greatly reduces the amount of calculation and will provide a method for tackling the evaluation of the anomalous dimensions of other operators.

As is well known the mass anomalous dimension coincides with the anomalous dimension of the mass operator $\bar{\psi}\psi$,

$$\gamma_m = \gamma_{\bar{\psi}\psi} + 2\gamma_\psi . \quad (6.1)$$

Here γ_ψ is the quark anomalous dimension and the RG function $\gamma_{\bar{\psi}\psi}$ is expressed via the renormalization constant of the mass operator by

$$\gamma_{\bar{\psi}\psi} = M\partial_M \ln Z_{\bar{\psi}\psi} , \quad [\bar{\psi}\psi]_R = Z_{\bar{\psi}\psi} Z_\psi^{-2} [\bar{\psi}_0\psi_0]_0 . \quad (6.2)$$

To determine the renormalization constant $Z_{\bar{\psi}\psi}$ at second order in the $1/N_f$ expansion one has to compute the divergences of the one-particle irreducible 2-point Green function with the insertion of the mass operator. The corresponding diagrams can be obtained from the diagrams contributing to the quark self-energy of figure 2 by the insertion of a $\bar{\psi}\psi$ vertex in the quark lines connecting the external vertices. At the level of diagrams this equivalent to the insertion of the unit operator in a fermion line

$$\frac{\not{p}}{p^2} \rightarrow \frac{\not{p}}{p^2} \cdot \frac{\not{p}}{p^2} .$$

As was discussed in section 4 the differentiation of the propagator diagrams with respect to p_μ , where p is the external momentum, results in the same set of the diagrams as for the mass operator. The only difference is that the inserted vertex in this case is $(-\gamma_\mu)$. We shall exploit this fact and show below that provided the Landau gauge is used then the corresponding contributions to $Z_1 = Z_\psi^2$ and $Z_{\bar{\psi}\psi}$ from all diagrams from both sets, except for two which arise from graphs (b) and (c) of figure 2 when the insertion of the new vertex is in the middle quark line, are related to one other by

$$Z_{\bar{\psi}\psi}^{(i)} = \frac{\mu Z_1^{(i)}}{(\mu - 2)} . \quad (6.3)$$

So given that γ_ψ is known then to determine the mass dimension γ_m at $O(1/N_f^2)$ it is sufficient to compute the contributions to Z_1 and $Z_{\bar{\psi}\psi}$ from the two extra diagrams. However, their calculation does not lead to any difficulties using the methods discussed in section 4.

We now proceed to the proof of the relation (6.3). First, we use the freedom we have to choose the external momentum flow in a diagram arbitrarily when calculating the contribution to the renormalization constants by directing the external momentum flow through the inserted vertex and out through the nearest external vertex. After this all the diagrams in question take the form shown in figure 12. All that one needs to know about the coloured block in figure 12 is its Lorentz structure,

$$\Gamma_\nu(q, \Delta) = \frac{1}{(q^2)^{n_i \Delta}} \left(\gamma_\nu A(\Delta) + \frac{q_\nu \not{q}}{q^2} B(\Delta) \right) , \quad (6.4)$$

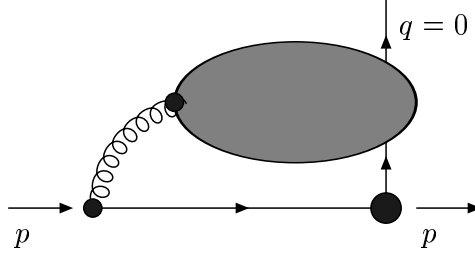


Figure 12: External momenta routing in the quark 2-point function with an operator insertion. The large black dot stands for the $V_i = \{I, (-\gamma_\mu)\}$.

where n_i is the number of the gluon lines in the block and the exact form of the functions $A(\Delta)$ and $B(\Delta)$ are irrelevant for our present discussion. Since the gluon propagator which joins this generalized vertex is purely transverse in the Landau gauge the second term in (6.4) will not contribute to the final answer. Thus the momentum integral for the diagram in figure 12 can be cast in the form

$$A(\Delta) \int \frac{d^{2\mu}q}{(2\pi)^{2\mu}} \frac{\gamma^\rho (\not{p} - \not{q}) V_i \gamma^\nu \not{q} P_{\rho\nu}^\perp(q)}{(p-q)^2 (q^2)^{\mu+(n_i+1)\Delta}}. \quad (6.5)$$

We are interested in the pole terms of this integral only, and bearing in mind that after the subtraction of the divergent subgraphs, which also have the same form, the latter is independent of p . Therefore one can rewrite (6.5) as

$$- A(\Delta) \left(V_i - \frac{1}{2\mu} \gamma_\rho \gamma_\nu V_i \gamma^\nu \gamma^\rho \right) \int \frac{d^{2\mu}q}{(2\pi)^{2\mu}} \frac{1}{(p-q)^2 (q^2)^{\mu-1-(n_i+1)\Delta}}, \quad (6.6)$$

where we have used the fact that up to p -dependent terms one can replace $q_\rho q_\nu$ by $q^2/(2\mu)$ in the integrand. It is easy to deduce that the combination in the prefactor in (6.6) is equal to $-(2\mu-1)$ for $V = I$, and to $(2\mu-1)(\mu-2)/\mu$ for $V = -\gamma_\mu$. Then one can immediately conclude that irrespective of the exact form of the constant $A(\Delta)$ which corresponds to the structure of the coloured block in figure 12, the contributions of the corresponding diagram to the renormalization constants Z_1 and $Z_{\bar{\psi}\psi}$ are indeed related by equation (6.3). To complete the calculation of γ_m one needs to compute the contributions from the graphs originating from those b, c in figure 2. These, as well as the determination of the graphs when the gluon propagator is taken in an arbitrary gauge, can readily be performed.

7 Discussion.

We are now in a position to assemble our results. First, using the formalism of section 3 we record that the d -dimensional expression for the quark anomalous dimension is

$$\begin{aligned} \gamma_\psi^{(2)} &= \frac{C_F \eta_0^2}{2(\mu-2)(2\mu-1)} \left[C_F \left(\frac{2(\mu-1)^2(\mu-3)}{\mu(\mu-2)} + 3\mu(\mu-1) \left(\Theta(\mu) - \frac{1}{(\mu-1)^2} \right) \right) \right. \\ &+ \frac{C_A}{2} \left(\frac{(12\mu^4 - 72\mu^3 + 126\mu^2 - 75\mu + 11)}{(2\mu-1)(2\mu-3)(\mu-2)} - \mu(\mu-1) (\Psi^2(\mu) + \Phi(\mu)) \right) \\ &+ \left. \frac{(8\mu^5 - 92\mu^4 + 270\mu^3 - 301\mu^2 + 124\mu - 12)\Psi(\mu)}{2(\mu-2)(2\mu-1)(2\mu-3)} \right] \end{aligned}$$

$$- \left. \frac{\xi(\mu^2 - 4\mu + 2)}{2(\mu - 1)(\mu - 2)} - \frac{\xi^2(2\mu^3 - 11\mu^2 + 12\mu - 4)}{4(\mu - 1)(\mu - 2)(2\mu - 1)} \right] . \quad (7.1)$$

We note that as an initial check on the result setting $C_F = 1$ and $C_A = 0$ one obtains the expression for the quark anomalous dimension of the abelian Thirring model. Again, in agreement with general results, [25], we find that in this case $\gamma_\psi^{(2)}$ is independent of the gauge fixing parameter. Further, collecting all the results for the quark mass anomalous dimension, we find

$$\begin{aligned} \gamma_{m,2} = & - 2 \left[\frac{2(\mu - 1)^2(\mu - 3)}{\mu(\mu - 2)} + 3\mu(\mu - 1) \left(\Theta(\mu) - \frac{1}{(\mu - 1)^2} \right) \right. \\ & \left. + \frac{(2\mu^2 - 4\mu + 1)}{(\mu - 2)} \right] \frac{C_F^2 \eta_0^2}{(\mu - 2)^2(2\mu - 1)} \\ & - \left[\frac{(12\mu^4 - 72\mu^3 + 126\mu^2 - 75\mu + 11)}{(2\mu - 1)(2\mu - 3)(\mu - 2)} - \mu(\mu - 1) (\Psi^2(\mu) + \Phi(\mu)) \right. \\ & \left. + \frac{(8\mu^5 - 92\mu^4 + 270\mu^3 - 301\mu^2 + 124\mu - 12)\Psi(\mu)}{2(2\mu - 1)(2\mu - 3)(\mu - 2)} \right. \\ & \left. - \frac{\mu^2(2\mu - 3)^2}{4(\mu - 2)(\mu - 1)} \right] \frac{C_F C_A \eta_0^2}{(\mu - 2)^2(2\mu - 1)} , \quad (7.2) \end{aligned}$$

where $\gamma_m(g_*) = \sum_{r=1}^{\infty} \gamma_{m,r}/n^r$. We have performed the calculations with a non-zero gauge parameter to check that it cancels exactly since the mass dimension is a gauge independent quantity. Aside from the internal checks on the integration which we discussed earlier, there are other checks on the correctness of (7.1) and (7.2). First, the terms of (7.1) and (7.2) involving C_F^2 have both been derived previously in QED in [23] and [24] respectively. However, a more stringent check rests in the relation of the results with the critical renormalization group equation since the RG functions evaluated at g_* ought to agree with (7.1) and (7.2) at the same order in $1/N_f$ and $O(\epsilon^4)$. It is elementary to verify that our results are in agreement with the Landau gauge anomalous dimension of [8, 35]. Also the result for $\gamma_m(g_*)$ is consistent with [9, 11, 2, 3].

Having verified this agreement we can now determine new information on the structure of the renormalization group functions in principle to all orders in the strong coupling constant. However, we will record values of the coefficients to six loops by writing

$$\begin{aligned} \gamma(a) = & - \left(\frac{1}{4} T_F N_f + \frac{3}{16} C_F - \frac{25}{32} C_A \right) C_F a^2 \\ & + \left(320 T_F^2 N_f^2 + 432 C_F T_F N_f - 4592 C_A T_F N_f + 216 C_F^2 \right. \\ & \left. + (1728\zeta(3) - 5148) C_F C_A + (9155 - 1242\zeta(3)) C_A^2 \right) \frac{C_F a^3}{4608} \\ & + \sum_{r=4}^{\infty} \left(c_{r0} T_F^{r-1} N_f^{r-1} + c_{r1} T_F^{r-2} N_f^{r-2} \right) C_F a^r + O\left(\frac{1}{N_f^3}\right) \quad (7.3) \end{aligned}$$

for the Landau gauge and

$$\begin{aligned} \gamma_m(a) = & - \frac{3}{2} C_F a + \left(\frac{10}{24} T_F N_f - \frac{3}{16} C_F - \frac{97}{48} C_A \right) C_F a^2 \\ & + \sum_{r=3}^{\infty} \left(m_{r0} T_F^{r-1} N_f^{r-1} + m_{r1} T_F^{r-2} N_f^{r-2} \right) C_F a^r + O\left(\frac{1}{N_f^3}\right) \quad (7.4) \end{aligned}$$

for the mass dimension where the order symbol means that contributions which are third order in $1/N_f$ and $O(\epsilon^7)$ at criticality are ignored. Although the full four loop $\overline{\text{MS}}$ β -function is only

available it may seem that it is not possible to decode the Landau gauge information in (7.1) and (7.2) beyond four loops since this requires a_* to $O(\epsilon^6)$. However, recalling that we are computing within the $1/N_f$ expansion we can use the information contained in the QCD β -function exponent $\omega = -\beta'(a_*)/2$ which has been determined at $O(1/N_f)$ in [16]. From [16], we deduce that the relevant corrections are

$$\begin{aligned}
a_* &= \frac{3\epsilon}{T_F N_f} + \left[\frac{33}{4} C_A \epsilon - \left(\frac{27}{4} C_F + \frac{45}{4} C_A \right) \epsilon^2 + \left(\frac{99}{16} C_F + \frac{237}{32} C_A \right) \epsilon^3 \right. \\
&\quad + \left(\frac{77}{16} C_F + \frac{53}{32} C_A \right) \epsilon^4 - \frac{3}{256} [(288\zeta(3) + 214)C_F + (480\zeta(3) - 229)C_A] \epsilon^5 \\
&\quad - \frac{1}{256} [(3168\zeta(3) - 2592\zeta(4) - 1506)C_F \\
&\quad \quad \left. + (3792\zeta(3) - 4320\zeta(4) + 1359)C_A] \epsilon^6 + O(\epsilon^7) \right] \frac{1}{T_F^2 N_f^2} + O\left(\frac{1}{N_f^3}\right).
\end{aligned} \tag{7.5}$$

Therefore, with this value we deduce the new exact contributions to (7.3) and (7.4) are

$$\begin{aligned}
c_{40} &= \frac{35}{1296} \\
c_{41} &= \frac{C_F}{72} [19 - 18\zeta(3)] + \frac{C_A}{1152} [293 + 288\zeta(3)] \\
c_{50} &= \frac{1}{7776} [83 - 144\zeta(3)] \\
c_{51} &= \frac{C_F}{31104} [5616\zeta(3) - 3888\zeta(4) - 659] + \frac{C_A}{62208} [7776\zeta(4) - 8928\zeta(3) - 1783] \\
c_{60} &= \frac{1}{15552} [65 - 144\zeta(4) + 80\zeta(3)] \\
c_{61} &= \frac{C_F}{46656} [4212\zeta(4) - 2592\zeta(5) - 432\zeta(3) - 2219] \\
&\quad + \frac{C_A}{31104} [4608\zeta(5) - 1440\zeta(4) - 4744\zeta(3) - 925]
\end{aligned} \tag{7.6}$$

and

$$\begin{aligned}
m_{50} &= \frac{5\zeta(3)}{162} - \frac{\zeta(4)}{18} + \frac{65}{2592} \\
m_{51} &= \left[\frac{5\zeta(4)}{8} - \frac{\zeta(5)}{3} - \frac{11\zeta(3)}{48} - \frac{4483}{20736} \right] C_F \\
&\quad + \left[\frac{8\zeta(5)}{9} - \frac{17\zeta(4)}{36} - \frac{671\zeta(3)}{1296} - \frac{18667}{124416} \right] C_A \\
m_{60} &= \frac{1}{46656} [560\zeta(3) + 720\zeta(4) - 1728\zeta(5) + 451] \\
m_{61} &= \frac{C_F}{186624} [46704\zeta(3) - 23328\zeta(4) + 51840\zeta(5) - 41472\zeta^2(3) - 25920\zeta(6) - 12283] \\
&\quad + \frac{C_A}{186624} [56728\zeta(3) - 59472\zeta(4) - 112896\zeta(5) + 55296\zeta^2(3) + 112320\zeta(6) - 22709].
\end{aligned} \tag{7.8}$$

We have given the explicit expression for c_{41} in order to compare with the full $\overline{\text{MS}}$ gauge calculation of [35] which was carried out for the particular colour group $SU(N_c)$ and note exact agreement. Further, we note that in [19] it was pointed out how the asymptotic Padé approximant predictions of [36] for m_{50} and m_{51} compared with the exact values we have determined.

Although we have concentrated on the relation of our results to four dimensional perturbation theory, we can also quote values of the exponents in three dimensions. These will be important for alternative critical point investigations of the non-abelian Thirring model and QCD equivalence, such as the lattice. For the wave function, we find from (7.1)

$$\eta = \frac{4C_F(3\xi - 2)}{3\pi^2 T_F N_f} + \frac{8C_F}{9\pi^4 T_F^2 N_f^2} \left[(64 - 6\pi^2) C_F + (8\xi^2 + 14\xi - 18 - \pi^2) C_A \right] + O\left(\frac{1}{N_f^3}\right). \quad (7.9)$$

However, for the physically more interesting mass exponent we deduce,

$$\gamma_m = -\frac{32C_F}{3\pi^2 T_F N_f} + \frac{32C_F[(56 - 6\pi^2)C_F - (18 + \pi^2)C_A]}{9\pi^4 T_F^2 N_f^2} + O\left(\frac{1}{N_f^3}\right). \quad (7.10)$$

It would be interesting to see how the numerical values of these exponents compare with the lattice. Indeed the dominant contribution from the $O(1/N_f^2)$ correction in the latter exponent arises from the C_A term.

In conclusion we have provided an elegant alternative to computing perturbative information on QCD at a new order in the large N_f expansion. Although the evaluation of the Feynman integrals has formed a significant part of the discussion, is technically quite involved and provides useful techniques for future massless integral evaluation, we believe we have demonstrated that the computation of other renormalization group functions in QCD is viable in principle. An example of this is the twist-2 operators which arise in deep inelastic scattering. Furthermore, the relation of the NATM to QCD has been put on a firmer ground. Indeed we believe that this critical relation between both models deserves further investigation.

Acknowledgements. This work was carried out with the support of the Russian Foundation of Basic Research, Grant 97-01-01152 (SED and ANM), by DFG Project N KI-623/1-2 (SED), a University of Pisa Exchange Research Fellowship (MC), PPARC through an Advanced Fellowship (JAG) and GSI (ANM). Also SED and ANM would like to thank Prof. A.N. Vasil'ev for useful discussions. Invaluable to the calculations were the symbolic manipulation programme FORM, [37], and computer algebra package REDUCE, [38].

A Basic integration rules.

In this appendix we give formulæ for the Fourier transformation, integration of chains and uniqueness relations for the vertices of different type. The following notation is used. We define

$$a(x_1, \dots, x_n) = \prod_{i=1}^n a(x_i)$$

where $a(\alpha) = \Gamma(\alpha')/\Gamma(\alpha)$ with $\alpha' = (\mu - \alpha)$. The Fourier transforms of various functions are given by

$$\int d^{2\mu}x \frac{e^{ipx}}{(x^2)^\alpha} = \pi^\mu a(\alpha) \frac{2^{2\alpha'}}{(p^2)^{\alpha'}}$$

$$\int d^2\mu x e^{ipx} \frac{x_\nu}{(x^2)^{\alpha+1}} = i\pi^\mu 2^{2\alpha'-1} \frac{a(\alpha)}{\alpha} \frac{p_\nu}{(p^2)^{\alpha'}}$$

$$\int d^2\mu x e^{ipx} \frac{x_\mu x_\nu}{(x^2)^{\alpha+1}} = \pi^\mu \frac{a(\alpha)}{\alpha} \frac{2^{2\alpha'-1}}{(p^2)^{\alpha'}} \left[\eta_{\mu\nu} - 2\alpha' \frac{p_\mu p_\nu}{p^2} \right] \quad (\text{A.1})$$

$$\int d^2\mu x e^{ipx} \frac{x_\mu x_\nu x_\rho}{(x^2)^{\alpha+1}} = i\pi^\mu a(\alpha) \frac{\alpha'}{\alpha} \frac{2^{2\alpha'}}{(p^2)^{\alpha'+1}} \left[p_\mu \eta_{\nu\rho} + p_\nu \eta_{\mu\rho} + p_\rho \eta_{\mu\nu} - 2(\alpha' + 1) \frac{p_\mu p_\nu p_\rho}{p^2} \right]$$

$$\int d^2\mu x \frac{e^{ipx}}{(x^2)^\alpha} \left[\eta_{\mu\nu} - \frac{2x_\mu x_\nu}{x^2} \right] = \pi^\mu \frac{a(\alpha)}{\alpha} \frac{2^{2\alpha'}}{(p^2)^{\alpha'}} \left[(\alpha - 1) \eta_{\mu\nu} + 2\alpha' \frac{p_\mu p_\nu}{p^2} \right]$$

$$\int \frac{d^2\mu k}{(2\pi)^{2\mu}} e^{ipx} \frac{P_{\mu\nu}^\perp}{(k^2)^\alpha} = \frac{(2\alpha - 1) a(\alpha)}{(4\pi)^\mu} \frac{2^{2\alpha'-1}}{\alpha} \frac{1}{(x^2)^{\alpha'}} \left(\eta_{\mu\nu} + \frac{2\alpha'}{(2\alpha - 1)} \frac{x_\mu x_\nu}{x^2} \right). \quad (\text{A.2})$$

The integration of the basic chain with various tensor generalizations are given by

$$\int \frac{d^2\mu x}{\pi^\mu} \frac{1}{((z-x)^2)^\alpha (x^2)^\beta} = \frac{a(\alpha, \beta, \alpha' + \beta')}{z^{2(\alpha+\beta-\mu)}},$$

$$\int \frac{d^2\mu x}{\pi^\mu} \frac{x_\nu}{((z-x)^2)^\alpha (x^2)^\beta} = \frac{a(\alpha, \beta, \alpha' + \beta') \beta'}{\alpha' + \beta'} \frac{z_\nu}{(z^2)^{\alpha+\beta-\mu}},$$

$$\int \frac{d^2\mu x}{\pi^\mu} \frac{x_\nu (z-x)_\mu}{((z-x)^2)^\alpha (x^2)^\beta} = - \frac{\alpha' \beta' a(\alpha, \beta, \alpha' + \beta' + 1)}{2(\alpha' + \beta' + 1) (z^2)^{\alpha+\beta-\mu-1}} \left[\delta_{\mu\nu} + 2(\alpha' + 1 - \beta) \frac{z_\mu z_\nu}{z^2} \right],$$

$$\int \frac{d^2\mu x}{\pi^\mu} \frac{\not{x}(\not{z} - \not{x})}{((z-x)^2)^\alpha (x^2)^\beta} = - \alpha' \beta' a(\alpha, \beta, \alpha' + \beta' + 1) \frac{1}{(z^2)^{\alpha+\beta-\mu-1}}, \quad (\text{A.3})$$

$$\int \frac{d^2\mu x}{\pi^\mu} \frac{1}{((z-x)^2)^\alpha (x^2)^\beta} \left[A \delta_{\mu\nu} + B \frac{x_\mu x_\nu}{x^2} \right]$$

$$= \frac{a(\alpha, \beta, \alpha' + \beta')}{(z^2)^{\alpha+\beta-\mu}} \left[\left(A + \frac{B\alpha'}{2\beta(\alpha' + \beta')} \right) \delta_{\mu\nu} + \frac{B\beta'(\alpha - \beta')}{\beta(\alpha' + \beta')} \frac{z_\mu z_\nu}{z^2} \right]. \quad (\text{A.4})$$

Next we list the uniqueness relations for the three type of vertices which arose in our calculations where the appropriate uniqueness value for each vertex is recorded in parentheses beside each rule.

Boson vertex ($\alpha + \beta + \gamma = 2\mu$).

$$\begin{array}{c} \gamma \\ | \\ \bullet \\ / \quad \backslash \\ \alpha \quad \beta \end{array} = \pi^\mu a(\alpha, \beta, \gamma) \quad \begin{array}{c} \beta' \quad \alpha' \\ \triangle \\ \gamma' \end{array}$$

Gross-Neveu vertex ($\alpha + \beta + \gamma = 2\mu - 1$).

$$\begin{array}{c} \gamma \\ | \\ \bullet \\ / \quad \backslash \\ \alpha + 1 \quad \beta + 1 \end{array} = \pi\mu \frac{a(\alpha, \beta, \gamma)}{\alpha\beta} \begin{array}{c} \beta' \quad \alpha' \\ \triangle \\ \gamma' \end{array}$$

Vector-fermion vertex ($\alpha + \beta + \gamma = 2\mu - 1$).

$$\begin{array}{c} x, \nu \\ | \\ \text{wavy} \\ | \\ \bullet \\ / \quad \backslash \\ \alpha + 1 \quad \beta + 1 \\ y \quad z \end{array} = \pi\mu \frac{a(\alpha, \beta, \gamma)}{\alpha\beta\gamma} \left\{ \begin{array}{c} \beta' \quad \alpha' \\ \triangle \\ \gamma' \end{array} \times (\gamma - 1) + 2\gamma' \times \frac{\Lambda_\nu^x(z, y)}{\gamma' + 1} \begin{array}{c} \beta' - 1 \quad \alpha' - 1 \\ \triangle \\ \gamma' + 1 \end{array} \right\}$$

Here

$$\Lambda_\nu^x(z, y) = \frac{(z-x)_\nu}{(z-x)^2} - \frac{(y-x)_\nu}{(y-x)^2}.$$

As usual the line with an arrow with index α denotes the fermion propagator, $\not{x}/(x^2)^\alpha$, a simple line corresponds to the boson propagator $1/(x^2)^\alpha$ and a wavy one is used to denote the conformal propagator (4.4).

B Renormalization constants.

In this appendix we collect the values of the renormalization constants Z_i and the basic RG functions at $O(1/N_f)$. The calculations are rather straightforward and so we only list the results.

We found

$$\begin{aligned} Z_1 &= 1 - \frac{gC_F\eta_0}{2n\Delta} \left(1 + \frac{\xi\mu}{(2\mu-1)(\mu-2)} \right) \\ Z_2 &= 1 - \frac{g\eta_0}{2n\Delta} (C_F - C_A/2) \left(1 + \frac{\xi\mu}{(2\mu-1)(\mu-2)} \right) - \frac{g^2C_A\eta_0}{8n\Delta} \left(\frac{\mu-1+\xi}{\mu-2} \right) \\ Z_3 &= 1 + \frac{g\lambda^2C_A\eta_0}{4n\Delta(\mu-2)} \left(1 - \frac{\xi}{(2\mu-1)} \right) \\ Z_4 &= 1 - \frac{g\xi\lambda C_A\eta_0}{8n(\mu-2)\Delta} \left(\frac{\lambda}{(2\mu-1)} + \frac{g}{2} \right) \end{aligned} \quad (\text{B.1})$$

where

$$\eta_0 = \frac{(\mu-2)(2\mu-1)\Gamma(2\mu)}{\Gamma^2(\mu)\Gamma(\mu+1)\Gamma(2-\mu)} \quad (\text{B.2})$$

and g is defined in (3.12). Using (3.13), (3.14) and (3.7) one finds

$$\eta^{(1)} = 2\gamma_\psi^{(1)} = C_F\eta_0 \left(1 + \frac{\xi\mu}{(2\mu-1)(\mu-2)} \right) \quad (\text{B.3})$$

$$\gamma_c^{(1)} = -\frac{C_A\eta_0}{4(\mu-2)}\left(1 - \frac{\xi}{(2\mu-1)}\right) \quad (\text{B.4})$$

$$\gamma_A^{(1)} = \frac{C_A\eta_0}{2(\mu-2)}\left(1 + \frac{\xi(\mu-1)}{(2\mu-1)}\right) \quad (\text{B.5})$$

For β_λ we obtain

$$\beta_\lambda = \lambda(\gamma_A + 2\gamma_c - \gamma_4) = \frac{\lambda(\lambda-1)C_A\eta_0}{4(\mu-2)(2\mu-1)}\left[\lambda(\xi - 2(2\mu-1)) - 2(\mu-1)\left(\xi + \frac{(2\mu-1)}{(\mu-1)}\right)\right]. \quad (\text{B.6})$$

One can see that $\lambda = 1$ is indeed a zero of the beta function. Also, for ξ_A we find

$$\xi_A^{(1)} = -\frac{(2\mu-1)}{(\mu-1)} \quad (\text{B.7})$$

and β_λ is simplified in this gauge to

$$\beta_\lambda = -\frac{(2\mu-1)C_A\eta_0}{4(\mu-2)(\mu-1)}\lambda^2(\lambda-1). \quad (\text{B.8})$$

Finally, for completeness we record the value of the amplitude combination \tilde{z} required in the SD formalism at $O(1/N_f^2)$. It is

$$\tilde{z}_1 = \frac{\Gamma(\mu+1)\eta_0}{2(2\mu-1)(\mu-2)} \quad (\text{B.9})$$

and

$$\begin{aligned} \tilde{z}_2 = & \frac{3\mu(\mu-1)\Gamma(\mu+1)C_F\eta_0^2}{2(2\mu-1)^2(\mu-2)^2}\left[\Theta(\mu) - \frac{1}{(\mu-1)^2}\right] \\ & + \frac{\mu(\mu-1)\Gamma(\mu+1)C_A\eta_0^2}{4(2\mu-1)^2(\mu-2)^2}\left[3\Theta(\mu) + \frac{(8\mu^5 - 92\mu^4 + 270\mu^3 - 301\mu^2 + 124\mu - 12)\Psi(\mu)}{2\mu(\mu-1)(2\mu-1)(2\mu-3)(\mu-2)}\right. \\ & - \Psi^2(\mu) - \Phi(\mu) + \frac{\bar{\xi}^2}{4(\mu-1)^2} + \frac{(\mu^2 + 2\mu - 2)\bar{\xi}}{2(\mu-1)^2\mu^2} \\ & \left. - \frac{(16\mu^7 - 120\mu^6 + 420\mu^5 - 776\mu^4 + 742\mu^3 - 349\mu^2 + 84\mu - 12)}{2(2\mu-1)(2\mu-3)(\mu-1)^2(\mu-2)\mu^2}\right] \quad (\text{B.10}) \end{aligned}$$

where the gluon propagator in the SD formalism is taken as

$$\tilde{A}_{\mu\nu}(k) = \frac{\tilde{B}}{(k^2)^{\mu-\beta}}\left[\eta_{\mu\nu} - (1-\bar{\xi})\frac{k_\mu k_\nu}{k^2}\right] \quad (\text{B.11})$$

in momentum space. These will be useful in the calculation of gauge independent critical exponents at $O(1/N_f^2)$. For example, if one chooses a particular gauge to simplify those calculations, such as the Feynman gauge used in standard perturbative calculations, then one will require the value of the relevant variables for a general gauge parameter.

References.

- [1] T. van Ritbergen, J.A.M. Vermaseren & S.A. Larin, Phys. Lett. **B400** (1997), 379.
- [2] J.A.M. Vermaseren, S.A. Larin & T. van Ritbergen, Phys. Lett. **B405** (1997) 327.
- [3] K.G. Chetyrkin, Phys. Lett. **B404** (1997) 161.
- [4] D.J. Gross & F.J. Wilczek, Phys. Rev. Lett. **30** (1973) 1343; H.D. Politzer, Phys. Rev. Lett. **30** (1973) 1346.
- [5] W.E. Caswell, Phys. Rev. Lett. **33** (1974) 244; D.R.T. Jones, Nucl. Phys. **B75** (1974) 531.
- [6] E.S. Egorian & O.V. Tarasov, Theor. Math. Phys. **41** (1979) 26.
- [7] O.V. Tarasov, A.A. Vladimirov & A.Yu. Zharkov, Phys. Lett. **B93** (1980) 429.
- [8] S.A. Larin & J.A.M. Vermaseren, Phys. Lett. **B303** (1993) 334.
- [9] D.V. Nanopoulos & D.A. Ross, Nucl. Phys. **B157** (1979) 273.
- [10] R. Tarrach, Nucl. Phys. **B183** (1981) 384; O. Nachtmann & W. Wetzel, Nucl. Phys. **B187** (1981) 333.
- [11] O. Tarasov, JINR preprint P2-82-900.
- [12] A.N. Vasil'ev, Yu.M. Pis'mak & J.R. Honkonen, Theor. Math. Phys. **46** (1981) 157; Theor. Math. Phys. **47** (1981) 291.
- [13] A.N. Vasil'ev, Yu.M. Pis'mak & J.R. Honkonen, Theor. Math. Phys. **50** (1982) 127.
- [14] A.N. Vasil'ev & M.Yu. Nalimov, Theor. Math. Phys. **56** (1982) 643.
- [15] J.A. Gracey, Phys. Lett. **B318** (1993) 177.
- [16] J.A. Gracey, Phys. Lett. **B373** (1996) 178.
- [17] J.A. Gracey, Phys. Lett. **B322** (1994) 141; J.A. Gracey, Nucl. Phys. **B480** (1996) 73; J.F. Bennett & J.A. Gracey, Nucl. Phys. **B517** (1998) 241.
- [18] A. Hasenfratz & P. Hasenfratz, Phys. Lett. **B297** (1992) 166.
- [19] M. Ciuchini, S.É. Derkachov, J.A. Gracey & A.N. Manashov, Phys. Lett. **B458** (1999), 117.
- [20] S.É. Derkachov & A.N. Manashov, Nucl. Phys. **B522** (1998) 301.
- [21] S.É. Derkachov & A.N. Manashov, Theor. Math. Phys. **116** (1998) 379.
- [22] J.A. Gracey, J. Phys. **A24** (1991) L431.
- [23] J.A. Gracey, Nucl. Phys. **B414** (1994) 614.
- [24] J.A. Gracey, Phys. Lett. **B317** (1993) 415.
- [25] J. Zinn-Justin, *Quantum Field Theory and Critical Phenomena* (Clarendon, Oxford, 1990).
- [26] A.N. Vasil'ev, M.M. Perekalin & Yu.M. Pis'mak, Theor. Math. Phys. **55** (1982) 323.

- [27] A.N. Vasil'ev, M.M. Perekalin & Yu.M. Pis'mak, *Theor. Math. Phys.* **60** (1984) 317.
- [28] J.A. Gracey, *Int. J. Mod. Phys.* **A8** (1993) 2465.
- [29] A.A. Slavnov, *Nucl. Phys.* **B31** (1971) 301.
- [30] A.N. Vasil'ev & A.S. Stepanenko, *Theor. Math. Phys.* **94** (1982) 127.
- [31] D.I. Kazakov, *Phys. Lett.* **B133** (1983) 406.
- [32] A.N. Vasil'ev, Yu.M. Pis'mak & J.R. Honkonen, *Theor. Math. Phys.* **48** (1981) 750.
- [33] S.G. Gorishnii & A.P. Isaev, *Theor. Math. Phys.* **62** (1985), 232.
- [34] P. Ramond, *Field Theory: A Modern Primer* *Frontiers in Physics Lecture Note Series* 51 (Benjamin Cummings, Reading MA, 1981).
- [35] K.G. Chetyrkin & A. R etey, hep-ph/9910332.
- [36] J. Ellis, I. Jack, D.R.T. Jones, M. Karliner & M.A. Samuel, *Phys. Rev.* **D57** (1998) 2665.
- [37] J.A.M. Vermaseren, "FORM" version 2.3, CAN publication, (1991).
- [38] A.C. Hearn, "REDUCE Users Manual" version 3.4, Rand publication CP78, (1991).